

Computationally efficient guaranteed cost control design for homogeneous clustered networks. [★]

B. Adhikari ^{a,1}, J. Veetaseveera ^{a,1}, V.S. Varma ^{a,b}, I.-C. Morarescu ^{a,b} E. Panteley ^c

^aUniversité de Lorraine, CNRS, CRAN, F-54000 Nancy, France

^bassociated with Automation Department, Technical University of Cluj-Napoca

^cL2S, CNRS, CentraleSupélec, Université Paris-Saclay, 91192 Gif-sur-Yvette, France.

Abstract

We consider a clustered network where connections inside the cluster are dense and between clusters are sparse. This leads us to a classical decoupling into fast (intra-cluster) and slow (inter-cluster) dynamics. Our objective is to provide a computationally efficient method to design control strategies that guarantee a certain bound on the cost for each cluster. Basically, we design a composite synchronizing controller with two terms: one responsible for the intra-cluster synchronization and the other achieving the synchronization between clusters. The first one does not require much computational effort since an analytic expression describes it. The second term is designed through a satisfaction equilibrium approach. In other words, the internal (fast) and external (slow) controllers are independently designed, and they ensure a guaranteed satisfactory cost for each cluster. Moreover, we show that the internal control affects the cluster cost only for a short time period. Finally, numerical simulations illustrate the theoretical results.

Key words: Synchronization; Distributed Control; Networked System; Singular Perturbation; Time-Scale Modeling; Clustered Network

1 Introduction

Due to its application in various domains such as power systems [11], wireless sensor networks [25], social networks [32], and biology [4], analysis and control of network synchronization have received significant attention in the literature. A particular case of the networked system is *clustered network*, where the network is divided into distinct groups (*clusters*) and the communication inside these groups is dense while the communication between these groups is sparse, see e.g. [22]. A typical example that falls into this framework is power systems. The increase in the number of interconnections and interchanges of energy in the electrical networks cause these low-frequency oscillations where a group of generators oscillates relative to each other known as *inter-area oscillation*. A decentralized control can be used to dampen these oscillations and stabilize the network. But

decentralized control on the one hand can interact in adverse ways and destabilize the overall system and on the other hand, even if it provides stability it may result in poor performance [16]. An alternative approach would be to design control based on global information but this comes with a large computational burden that increases with the size of the network. In such scenarios, a control design approach that classifies the system with coherent dynamics into a group i.e., *clusters* and divides the design problem into smaller sub-problems can be an effective approach. Motivated by such scenarios, in this paper, we study the design of an efficient control scheme for the clustered network. In power networks, the group of generators that oscillate against each other can be classified into clusters and an efficient system analysis can be performed. Networks with such properties also appear in various disciplines, such as energy systems [28], physics [2], [30], biological systems [13], social networks [7], [12] etc.

A majority of the publication on clustered networks propose an analysis of networks in consensus framework, see e.g. [9], [8], [24]; while the problem of control design is less common in such a setting. A particular setup for synchronizing clustered networks using two time-scales is considered in [5], [27]. In [5], the authors expressed the consensus problem in terms of the synchronization problem and

[★] This work was partially funded by CEFIPRA through the project number 6001-1, by ANR under grants HANDY ANR-18-CE40-0010 and NICETWEET ANR-20-CE48-0009 and by the PNRR project DECIDE No. 760069.

Email addresses: bikas3121@gmail.com (B. Adhikari), jomphopv@hotmail.fr (J. Veetaseveera).

¹ B. Adhikari and J. Veetaseveera contributed equally to this work as first authors while working at CRAN.

proposed a computationally efficient control design strategy using time-scale separation. A distributed two-time-scales consensus algorithm is presented in [27] with an explicit formula for the convergence rate. However, none of the previously mentioned works consider the problem where the control objective has a cost optimization requirement in addition to synchronization. On the one hand, these requirements are timely, and on the other, induce a high computational load, preventing the design of (sub-)optimal controllers in a centralized manner.

A major problem related to the synchronization of large-scale networks is the computational load associated with the design of effective controllers. The cost related to the synchronization is either considered to be global or not considered at all in most of the existing literature, for example in [17], [6]. In [17], the authors propose an energy-aware controller to minimize a global cost consisting of communication and controller parts. The control design with optimal global cost in the framework of multi-agent systems is presented in [6]. The computational effort required is very high, and the problem is NP-hard due to the information structure imposed by the graph.

A computationally efficient decentralized control design approach is presented with global cost guarantees in [3]; however, the assumption of the same gain for all the agents in the network is quite restrictive. This obstacle in [3] was removed in [31] with individual cost guarantees for each agent. The proposed strategy works well with small-scale networks; however, the computational effort required to obtain the gain is huge for large-scale networks. In this paper, we aim to address this problem and provide an effective control design strategy for large-scale networks that reduces the computational effort while satisfying the performance guarantees.

One methodology to address the synchronization of the large-scale networks is by model reduction, which is based on *Singular Perturbation Theory (SPT)* that exploits the time-scale properties of clustered networks. The objective is to decrease the size of the system state while approximating its overall dynamic behavior. To the best of our knowledge, the first time-scale analysis of the networked system dates back to the 1980s, see [9], [10]. In these publications, the consensus problem for linear systems was analyzed using a singular perturbation approach under the assumption that graphs were undirected. Later on, these results were extended in [8] to nonlinear networks. Furthermore, the results from [9], [10] for the case time-varying directed graphs are extended in [24]. In the synchronization framework, singular perturbation analysis of heterogeneous network with fixed topology is presented in [23] and for the time-varying case in [1].

In this paper, we consider a problem of distributed controller design for a *homogeneous clustered network* that ensures synchronization of the overall network while optimizing some cost functions. We provide an approach that signif-

icantly reduces the computational effort required to obtain the controller by exploiting the clustered network structure. The dense interconnections result in a fast convergence inside the cluster toward a local agreement, and then slowly toward the global consensus. We use this property to divide the control design problem into computationally tractable sub-problems using *Time-Scale Separation (TSS)*. The fast variables represent the synchronization error inside the clusters, whereas the slow variables represent the aggregate behavior of the agent states within each cluster.

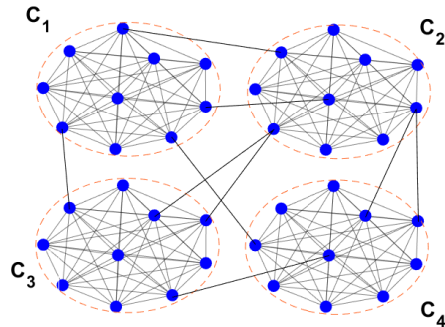


Fig. 1. A network partitioned into 4 clusters.

The design of our controller is based on the two-time-scales behavior of the clustered network. First, we perform the *Time-Scale Modeling (TSM)* to represent the network dynamics in *Standard Singular Perturbation Form (SSPF)*. As a result of TSM, internal control is associated with fast dynamics, while external control is associated with slow dynamics. Then, using time-scale separation, we decouple the dynamics into slow and fast subsystems and this decoupling allows us to design the internal and the external controller independently. The internal controller, associated with the fast dynamics, is designed to achieve a consensus inside the cluster while minimizing an internal cost. Since the convergence of agents inside the cluster towards the consensus is fast; the cluster roughly merges into a single node after the fast transient and external behavior is defined by the slow dynamics. The long-term behavior of the network depends on this slow dynamics. Finally, the external control is designed to synchronize all the clusters based on the satisfaction equilibrium approach [31], i.e., external control is designed such that the external cost associated with each cluster is bounded under a given threshold. In addition, we also provide an approximation of the cluster cost as a sum of the internal and external costs associated with internal and external control, respectively.

The main contributions of this paper can be outlined as follows, (1) we formulate a singular perturbation model of the clustered network using time-scale modeling in the synchronization framework, where each agent has its individual dynamics, (2) based on the obtained model in (1), we propose a computationally efficient sub-optimal control design scheme that synchronizes the network by splitting the controllers into two parts corresponding to the slow and fast

dynamics, and (3) finally, we provide an approximation of the cluster cost bound that is induced by the time-scale decoupling approach.

The remainder of the paper is organized as follows. The model and the control objectives are stated in Section II. The time-scale modeling and decoupling into slow and fast dynamics using time-scale separation are described in detail in Section III. Then, the internal and external controller design procedures are developed in Section IV. In Section V, we provide an approximation of the cluster cost. Finally, numerical results are presented in Section VI before concluding in Section VII. To make the paper easily readable, the proofs are presented in the Appendix.

1.1 Notation and Preliminaries

The symbol \otimes represents the Kronecker product. Let $(x, y) \in \mathbb{R}^{n+m}$ stand for $[x^\top y^\top]^\top$. The identity matrix of size n is denoted by I_n and by $\mathbb{1}_n \in \mathbb{R}^n$, the column vector whose components are all 1. For a matrix $A \in \mathbb{R}^{m \times n}$, A^\top denotes the transpose of A . For a vector $x \in \mathbb{R}^n$, we denote by $\|x\|_2 := \sqrt{x^\top x}$ its Euclidean norm and, for a matrix A , $\|A\|_2 := \sqrt{\lambda_{\max}(A^\top A)}$. For a square matrix $M \in \mathbb{R}^{n \times n}$, let $\lambda_{\min}(M)$ and $\lambda_{\max}(M)$ be the minimum and the maximum eigenvalue, respectively. The *measure of the square matrix* M is defined as $\nu(M) = \frac{1}{2} \lambda_{\max}(M + M^\top)$. We said that a matrix $M \in \mathbb{R}^{n \times n}$ is orthonormal if $M^\top M = M M^\top = I_n$. We denote by $M_{-k} \in \mathbb{R}^{(n-1) \times (n-1)}$ the matrix M with its k -th row and column removed. By $B = \text{diag}(B_1, \dots, B_N)$, we denote a block-diagonal matrix with the entries B_1, \dots, B_N on the diagonal and $B_{-k} := \text{diag}(B_1, \dots, B_{k-1}, B_{k+1}, \dots, B_N)$ the block-matrix with the k -th block removed. A vector function $f(t, \epsilon) \in \mathbb{R}^n$ is said to be $\mathcal{O}(\epsilon)$ over an interval $[t_1, t_2]$ if there exists positive constant k and ϵ^* such that $\|f(t, \epsilon)\| \leq k\epsilon$, for all $\epsilon \in [0, \epsilon^*]$, $\forall t \in [t_1, t_2]$, where $\|\cdot\|$ is the Euclidean norm [19]. A connected, undirected graph is represented as $\mathcal{G} = (\mathcal{V}, \mathcal{E})$, where $\mathcal{V} = \{1, 2, \dots, n\}$ is the agent set and $\mathcal{E} \subseteq \mathcal{V} \times \mathcal{V}$ is the edge set. The adjacency matrix $\mathcal{A} = (a_{ij})_{n \times n}$ is defined as: $a_{ij} \neq 0$ if $(j, i) \in \mathcal{E}$ and $a_{ij} = 0$, otherwise. The Laplacian of the graph \mathcal{G} is defined as \mathcal{L} , has $-a_{ij}$ off-diagonal elements and $\sum_{j=1}^n a_{ij}$ diagonal ones. Let $\mathbf{G} = (\mathcal{V}, \{\mathcal{K}_i\}_{i \in \mathcal{V}}, \{u_i\}_{i \in \mathcal{V}})$, be a strategic form game, where $\mathcal{V} = \{1, 2, \dots, n\}$ is the set of players (agents), \mathcal{K}_i is the set of strategies of the player i , and u_i is a utility function of the player i and $\{f_1, \dots, f_n\}$ be n set-valued satisfaction functions. Then the strategy profile $\mathcal{K}^* = (\mathcal{K}_1^*, \dots, \mathcal{K}_n^*)$ is a *Satisfaction Equilibrium (SE)* if and only if, for all $i \in \mathcal{V}$, we have, $\mathcal{K}_i^* \in f_i(\mathcal{K}_{-i}^*)$, where $\mathcal{K}_{-i}^* := (\mathcal{K}_1^*, \dots, \mathcal{K}_{i-1}^*, \mathcal{K}_{i+1}^*, \dots, \mathcal{K}_n^*)$ denotes the reduced profile with the component \mathcal{K}_i^* removed.

2 Problem Statement

2.1 Model Description

Consider a network of n agents partitioned into m non-empty clusters $\mathcal{C}_1, \dots, \mathcal{C}_m \subset \mathcal{V}$. Clustered network refers to a network that is divided into distinct groups of agents having dense connection structures, whereas the connections between the clusters are sparse. Let us denote by $\mathcal{M} = \{1, 2, \dots, m\}$, the set of clusters while n_k represents the cardinality of the cluster \mathcal{C}_k and $n = \sum_{k=1}^m n_k$. Each agent in the network is identified by a couple $(k, i) \in \mathcal{C}_k$, where, k refers to the cluster \mathcal{C}_k and i the index of the agent in the cluster \mathcal{C}_k . The notation $(k, j) \in \mathcal{N}_{k,i}$ represents the neighbors of the agent (k, i) in the same cluster \mathcal{C}_k . To each agent $(k, i) \in \mathcal{C}_k$, $k \in \mathcal{M}$, one assigns a state $x_{k,i} \in \mathbb{R}^{n_x}$ whose dynamics is

$$\dot{x}_{k,i} = Ax_{k,i} + Bu_{k,i}, \quad (1)$$

where $u_{k,i} \in \mathbb{R}^{n_u}$, $A \in \mathbb{R}^{n_x \times n_x}$ and $B \in \mathbb{R}^{n_x \times n_u}$. For each cluster \mathcal{C}_k , let $x_k := (x_{k,1}, \dots, x_{k,n_k}) \in \mathbb{R}^{n_k \cdot n_x}$ be the cluster state and $u_k := (u_{k,1}, \dots, u_{k,n_k}) \in \mathbb{R}^{n_k \cdot n_u}$ the cluster control. Thus, cluster dynamics takes the following form

$$\dot{x}_k = (I_{n_k} \otimes A)x_k + (I_{n_k} \otimes B)u_k, \quad \forall k \in \mathcal{M}. \quad (2)$$

Finally, the overall network dynamics take the following form,

$$\dot{x} = (I_n \otimes A)x + (I_n \otimes B)u, \quad (3)$$

where $x := (x_1, \dots, x_m) \in \mathbb{R}^{n \cdot n_x}$ and $u := (u_1, \dots, u_m) \in \mathbb{R}^{n \cdot n_u}$ are the network state and the network control, respectively.

The interactions between the agents in the network are encoded by the Laplacian matrix that can be written as $\mathcal{L} := \mathcal{L}^{int} + \mathcal{L}^{ext}$. The internal Laplacian of the network $\mathcal{L}^{int} := \text{diag}(\mathcal{L}_1^{int}, \dots, \mathcal{L}_m^{int})$ is a block-diagonal matrix, with each block \mathcal{L}_k^{int} referring to the Laplacian of the cluster \mathcal{C}_k excluding the external connections. The external Laplacian \mathcal{L}^{ext} represents the connections between agents from different clusters.

Moreover, we define a cluster cost J_k associated with each cluster \mathcal{C}_k , $k \in \mathcal{M}$, as

$$J_k = \int_0^{+\infty} x_k^\top(t) (\mathcal{L}_k^{int} \otimes I_{n_x}) x_k(t) + x^\top(t) (\mathcal{L}_k^{ext} \otimes I_{n_x}) x(t) + u_k^\top(t) (I_{n_k} \otimes R_k) u_k(t) dt, \quad (4)$$

where the internal Laplacian $\mathcal{L}_k^{int} \in \mathbb{R}^{n_k \times n_k}$ captures the connections inside the cluster \mathcal{C}_k , and the external Laplacian $\mathcal{L}_k^{ext} \in \mathbb{R}^{n_k \times n}$ expresses the external connections between \mathcal{C}_k and the neighboring clusters.

In the sequel, we consider the problem of network synchronization, and the network is said to be asymptotically synchronized for all $(k, i) \in \mathcal{C}_k$, $(l, j) \in \mathcal{C}_l$ and $k, l \in \mathcal{M}$, when $\lim_{t \rightarrow +\infty} \|x_{k,i}(t) - x_{l,j}(t)\| = 0$. The objective of the paper is to design a controller u while optimizing the cluster costs (4) for $k \in \mathcal{M}$,

Next, we state some assumptions on the network structure and the connectivity which are vital for the control design framework we are going to propose in this paper.

Assumption 1 *The overall graph and the graph of the cluster are undirected and connected.*

The assumption on the connectivity of the network in Assumption 1 provides the necessary condition for network synchronization. In addition, the graphs are also assumed to be unweighted. The following assumption on the dense intra-cluster communication, together with the adequate choice of the control gains, ensures that the synchronization inside the clusters is faster than between the clusters.

Assumption 2 *The internal graphs are very dense for all clusters, specifically, we assume that all non-zero eigenvalues for an internal Laplacian can be approximated by n_k i.e., for every cluster $k \in \mathcal{M}$, $\lambda_i(\mathcal{L}_k^{int}) \approx n_k$, $i = \{2, 3, \dots, n_k\}$.*

Remark 1 *In Assumption 2, the dense graph implies a type of graph in which the number of edges is close to the maximal number of edges. In real-world scenarios, the topology of the network may not be fully known or dynamically evolving to be able to determine the Laplacian eigenvalues. Even for the known graphs, the numerical computation of the eigenvalues may be impractical due to their sheer size. Thus, to address this difficulty and have the practical significance of our control design, we approximate the eigenvalues of the Laplacian matrices of the dense clusters by that of complete ones. Following the result in [15], this is justified because for large dense networks, the Laplacian matrix can be seen as a perturbation of the degree matrix of the graph and the contribution of the adjacency matrix to the Laplacian spectrum is small. This approach, on one hand, simplifies the control design while on the other hand, this simplification does not have a significant effect on the cost, which is validated using numerical results.*

2.2 Control Design Outline

For large networks, the control design problem under certain cost constraints becomes difficult as the computational complexity increases with an increase in network dimension. To simplify the calculations and minimize the computational efforts, for each cluster \mathcal{C}_k , $k \in \mathcal{M}$, we propose a composite control of the form:

$$u_k := u_k^{int} + u_k^{ext}, \quad \forall k \in \mathcal{M}, \quad (5)$$

where $u_k^{int} := (u_{k,1}^{int}, \dots, u_{k,n_k}^{int})$, $u_k^{ext} := (u_{k,1}^{ext}, \dots, u_{k,n_k}^{ext})$ and

$$\begin{cases} u_{k,i}^{int} := -K_k^{int} \sum_{(k,j) \in \mathcal{N}_{k,i}} (x_{k,i} - x_{k,j}), \\ u_{k,i}^{ext} := -K_k^{ext} \sum_{(l,p) \in \mathcal{N}_{k,i}} (x_{k,i} - x_{l,p}), \end{cases} \quad (6)$$

where $K_k^{int}, K_k^{ext} \in \mathbb{R}^{n_u \times n_x}$. The notation $(l, p) \in \mathcal{N}_{k,i}$ indicates the neighbors belonging to a different cluster, that is $l \neq k$. The internal control u_k^{int} is the effort required to achieve local agreement, whereas the external control u_k^{ext} is the energy necessary to synchronize the agents between the clusters.

Such a decomposition of the control allows us to decouple the overall optimization in the following way. Substituting the composite control (5), the cost function (4) can be written as the sum of internal, external, and a cross term as follows:

$$J_k = J_k^{int} + J_k^{ext} + J_k^{cross}, \quad (7)$$

where,

$$\begin{aligned} J_k^{int} &= \int_0^{+\infty} x_k^\top(t) (\mathcal{L}_k^{int} \otimes I_{n_x}) x_k(t) + u_k^{int \top}(t) (I_{n_k} \otimes R_k) u_k^{int}(t) dt, \\ J_k^{ext} &= \int_0^{+\infty} x_k^\top(t) (\mathcal{L}_k^{ext} \otimes I_{n_x}) x_k(t) + u_k^{ext \top}(t) (I_{n_k} \otimes R_k) u_k^{ext}(t) dt, \\ J_k^{cross} &= 2 \int_0^{+\infty} u_k^{ext \top}(t) (I_{n_k} \otimes R_k) u_k^{int}(t) dt. \end{aligned} \quad (8)$$

In this way, we replace the original problem of optimizing the cost function for the overall network given (4) with the problem of optimization of the internal and external costs. This way, the initial optimization problem is recast as a problem of finding the internal (K_k^{int}) and external (K_k^{ext}) control gains. The internal and external gains are designed independently, and the obtained internal gain is optimal while the external gain is sub-optimal because the internal cost is minimized and the external cost is capped below a certain threshold, respectively.

The next objective is to bound the total cluster cost with the sum of internal (J_k^{int}) and external (J_k^{ext}) cost and a constant term corresponding to the internal and external control. The cross term in the equation (8) can be bounded by a constant term multiplied by the norm of the initial conditions (See Theorem 2).

To solve this problem, we propose an approach based on time-scale separation that we describe in the following section.

3 Time-scale Separation

This section provides a procedure to decouple the closed-loop network dynamics into two subsystems, evolving on

different time-scales. First, we perform a coordinate transformation to exhibit the collective dynamics of the network: the average and the synchronization error dynamics. Then, we apply the TSS to decouple the collective dynamics into slow and fast subsystems. In two time-scale, the slow variable corresponds to the average of the agent's state while the fast variable corresponds to the synchronization error.

3.1 Coordinate Transformation

Let us consider the clusters without external connections. Then based on the internal Laplacian \mathcal{L}_k^{int} , following from [26], we introduce the coordinate transformation for the cluster \mathcal{C}_k . For a connected graph, the Jordan decomposition of the symmetric Laplacian matrix is,

$$\mathcal{L}_k^{int} = T_k \begin{bmatrix} 0 & 0 \\ 0 & \Lambda_k^{int} \end{bmatrix} T_k^\top, \quad \forall k \in \mathcal{M}, \quad (9)$$

where $T_k \in \mathbb{R}^{n_k \times n_k}$ is an orthonormal matrix and $\Lambda_k^{int} = \text{diag}(\lambda_{k,2}^{int}, \dots, \lambda_{k,n_k}^{int}) \in \mathbb{R}^{(n_k-1) \times (n_k-1)}$ collects the n_k-1 positive eigenvalues of \mathcal{L}_k^{int} . Moreover, the matrix T_k can be expressed as

$$T_k = \begin{bmatrix} v_{k,1} & V_k \end{bmatrix}, \quad \forall k \in \mathcal{M}, \quad (10)$$

where $v_{k,1}^\top = \frac{1}{\sqrt{n_k}} \mathbb{1}_{n_k}^\top$ is the eigenvector associated with the 0 eigenvalue and the matrix $V_k \in \mathbb{R}^{n_k \times (n_k-1)}$ contains the eigenvectors corresponding to the nonzero eigenvalues of \mathcal{L}_k^{int} . Furthermore, it can be verified that, $v_{k,1}^\top V_k = 0$ and $V_k^\top V_k = I_{n_k-1}$.

Now, we define the coordinate transformation as

$$\bar{x}_k := \begin{bmatrix} y_k \\ \xi_k \end{bmatrix} = \left(\frac{1}{\sqrt{n_k}} T_k^\top \otimes I_{n_x} \right) x_k, \quad \forall k \in \mathcal{M}. \quad (11)$$

Then, from (10) and (11), the change of variables yields, for all $k \in \mathcal{M}$,

$$y_k := \left(\frac{\mathbb{1}_{n_k}^\top}{n_k} \otimes I_{n_x} \right) x_k =: H_k x_k \in \mathbb{R}^{n_x} \quad (12)$$

$$\xi_k := \left(\frac{V_k^\top}{\sqrt{n_k}} \otimes I_{n_x} \right) x_k =: Z_k x_k \in \mathbb{R}^{(n_k-1) \cdot n_x}. \quad (13)$$

The first component y_k corresponds to the average of the respective agents' states in the cluster \mathcal{C}_k . In network synchronization, the synchronization error is defined as the difference between the individual state and the state of the averaged unit, i.e.,

$$e_k = x_k - \mathbb{1}_{n_k} y_k, \quad \forall k \in \mathcal{M}. \quad (14)$$

The second component, ξ_k corresponds to the projection of the synchronization error (14) as

$$\xi_k = Z_k x_k = Z_k (e_k + \mathbb{1}_{n_k} y_k) = Z_k e_k. \quad (15)$$

Since the matrix T_k is orthonormal i.e., $T_k^\top = T_k^{-1}$, the inverse of the transformation (11), for all $k \in \mathcal{M}$ yields,

$$\begin{aligned} x_k &= (\sqrt{n_k} T_k \otimes I_{n_x}) \bar{x}_k \\ &= (\mathbb{1}_{n_k} \otimes I_{n_x}) y_k + (\sqrt{n_k} V_k \otimes I_{n_x}) \xi_k \\ &=: \tilde{H}_k y_k + \tilde{Z}_k \xi_k. \end{aligned} \quad (16)$$

In vector form, let $x := (x_1, \dots, x_m) \in \mathbb{R}^{n \cdot n_x}$, $y := (y_1, \dots, y_m) \in \mathbb{R}^{m \cdot n_x}$ and $\xi := (\xi_1, \dots, \xi_m) \in \mathbb{R}^{(n-m) \cdot n_x}$, respectively. Then for the overall network, we obtain

$$y = Hx, \quad \xi = Zx \quad \text{and} \quad x = \tilde{H}y + \tilde{Z}\xi, \quad (17)$$

where $H = \text{diag}(H_1, \dots, H_m)$ and $Z = \text{diag}(Z_1, \dots, Z_m)$ and $\tilde{H} = \text{diag}(\tilde{H}_1, \dots, \tilde{H}_m)$ and $\tilde{Z} = \text{diag}(\tilde{Z}_1, \dots, \tilde{Z}_m)$. Now, we recast the overall network dynamics in terms of the new coordinate variables. The overall network dynamics in the presence of the control (5) is

$$\begin{aligned} \dot{x} &= ((I_n \otimes A) - (I_n \otimes B)K^{int}(\mathcal{L}^{int} \otimes I_{n_x}) \\ &\quad - (I_n \otimes B)K^{ext}(\mathcal{L}^{ext} \otimes I_{n_x}))x, \end{aligned} \quad (18)$$

where $K^{int} = \text{diag}((I_{n_1} \otimes K_1^{int}), \dots, (I_{n_m} \otimes K_m^{int}))$ and $K^{ext} = \text{diag}((I_{n_1} \otimes K_1^{ext}), \dots, (I_{n_m} \otimes K_m^{ext}))$. Then, using (17), the overall dynamics (18) is recast in new coordinates as follows,

$$\begin{cases} \dot{y} = \bar{A}_{11}y + \bar{A}_{12}\xi, \\ \dot{\xi} = \bar{A}_{21}y + (\bar{A}_{22}^1 + \bar{A}_{22}^2)\xi, \end{cases} \quad (19)$$

where,

$$\begin{cases} \bar{A}_{11} = ((I_m \otimes A) - H(I_n \otimes B)K^{ext}(\mathcal{L}^{ext} \otimes I_{n_x})\tilde{H}), \\ \bar{A}_{12} = -H(I_n \otimes B)K^{ext}(\mathcal{L}^{ext} \otimes I_{n_x})\tilde{Z}, \\ \bar{A}_{21} = -Z(I_n \otimes B)K^{ext}(\mathcal{L}^{ext} \otimes I_{n_x})\tilde{H}, \\ \bar{A}_{22}^1 = -Z(I_n \otimes B)K^{ext}(\mathcal{L}^{ext} \otimes I_{n_x})\tilde{Z}, \\ \bar{A}_{22}^2 = ((I_{n-m} \otimes A) - (I_n \otimes B)K_{n-m}^{int}(\Lambda^{int} \otimes I_{n_x})), \end{cases} \quad (20)$$

and $K_{n-m}^{int} = \text{diag}((I_{n_1-1} \otimes K_1^{int}), \dots, (I_{n_m-1} \otimes K_m^{int}))$ and $\Lambda^{int} = \text{diag}(\Lambda_1^{int}, \dots, \Lambda_m^{int})$. We recall that y and ξ correspond to the average of the agents' states and the synchronization error, respectively.

3.2 Network Dynamics in Two Time-scales

In the absence of agents' individual dynamics in [10], [24], the consensus dynamics is expressed in *Standard Singular Perturbation Form (SSPF)* based only on the density of connections inside and between the clusters. This was sufficient because the convergence required in [10] is dictated only by

the density of the connections in the consensus framework. However, in our case, the convergence towards synchronization manifold depends also on the control gains K^{int} and K^{ext} and we need to take them into account for the time-scale analysis i.e. while defining the network parameter (ϵ).

Thus, to study the time-scale behavior and analyze the synchronizing behavior, we define the network parameters as follows,

$$\begin{cases} \mu^{ext} := \|(I_n \otimes B)K^{ext}(\mathcal{L}^{ext} \otimes I_{n_x})\|, \\ \mu^{int} := \min_{k \in \mathcal{M}} \|(\Lambda_k^{int} \otimes BK_k^{int})\|, \\ \epsilon := \frac{\mu^{ext}}{\mu^{int}}. \end{cases} \quad (21)$$

The network parameter ϵ is the ratio of the strength of the controls between and within the clusters. It is worth noting that, in our case, the network parameter ϵ can be tuned by the choice of the control gains K^{ext} and K^{int} .

Remark 2 For the rest of this section, we assume that ϵ is small enough such that time-scale separation occurs, and the control design presented in the following section will serve, among others to ensure this property.

In the following, we analyze the order of the matrices in equation (20) with respect to the network parameters in equation (21).

Lemma 1 Let K^{ext} be designed such that $\|A\| \leq c_1 \mu^{ext}$, $c_1 > 0$, then the matrices in (20) satisfy the following conditions,

- $\|\bar{A}_{11}\|, \|\bar{A}_{12}\|, \|\bar{A}_{21}\|, \|\bar{A}_{22}^1\| \leq c_2 \epsilon \mu^{int}$,
- $\|\bar{A}_{22}^2\| \geq \mu^{int}$,

where $c_2 := c_1 + \sqrt{\bar{n}/\underline{n}}$, $\bar{n} = \max n_k$ and $\underline{n} = \min n_k$.

PROOF. See Appendix. \blacksquare

We here note that since μ^{ext} depends on K^{ext} , we can always choose K^{ext} sufficiently large such that the assumption of the Lemma 1 are satisfied. As a consequence of the Lemma 1 and by definition of the $\mathcal{O}(\epsilon)$ (see Notations), the ratio between the norm of the matrices $\bar{A}_{11}, \bar{A}_{12}, \bar{A}_{21}, \bar{A}_{22}^1$ with the norm of \bar{A}_{22}^2 are of order $\mathcal{O}(\epsilon)$. Since the dynamics of the variables y and ξ are dominated by the matrix \bar{A}_{11} and \bar{A}_{22}^2 , the variables y and ξ behaves as a slow and fast variables, respectively.

Now, to reveal the TSS, following the idea of [10], we re-scale the time with μ^{int} to obtain a fast time-scale as $t_f = \mu^{int}t$, and a slow time-scale $t_s = \epsilon t_f$. This allows us to represent the overall dynamics (19) in SSPF as follows,

$$\frac{dy}{dt_s} = A_{11}y + A_{12}\xi, \quad (22a)$$

$$\epsilon \frac{d\xi}{dt_s} = \epsilon A_{21}y + (\epsilon A_{22}^1 + A_{22}^2)\xi. \quad (22b)$$

where,

$$\begin{aligned} A_{11} &= \frac{\bar{A}_{11}}{\epsilon \mu^{int}}, & A_{12} &= \frac{\bar{A}_{12}}{\epsilon \mu^{int}}, & A_{21} &= \frac{\bar{A}_{21}}{\epsilon \mu^{int}}, \\ A_{22}^1 &= \frac{\bar{A}_{22}^1}{\epsilon \mu^{int}}, & A_{22}^2 &= \frac{\bar{A}_{22}^2}{\mu^{int}}. \end{aligned} \quad (23)$$

Next, we analyze the slow and fast dynamics of the singularly perturbed system (22).

3.3 Slow Dynamics

To define the slow dynamics of the system (22), we follow the standard approach of singular perturbation analysis [19]. Setting $\epsilon = 0$ in (22), we obtain that equation (22b) degenerates into equation $\xi_s(t_s) = 0$. Substituting this into equation (22a), we obtain the slow dynamics as

$$\frac{dy_s}{dt_s} = A_{11}y_s. \quad (24)$$

where y_s and ξ_s are the slow parts of the variables y and ξ , respectively. Equivalently, since $t_s = \epsilon t_f = \epsilon \mu^{int}t$, it yields,

$$\dot{y}_s(t) = (I_m \otimes A)y_s(t) + (I_m \otimes B)u_s(t), \quad (25)$$

where $u_s(t) = -HK^{ext}(\mathcal{L}^{ext} \otimes I_{n_x})\tilde{H}y_s(t)$. Notice that in our setting the slow dynamics (25) represents the collective behavior of the cluster and it may or may not be stable.

3.4 Fast Dynamics

Now, representing the dynamics (22) in fast time scale t_f and setting $\epsilon = 0$, we have $dy_f/dt_f = 0$ and we obtain the fast dynamics as follows,

$$\frac{d\xi_f}{dt_f} = A_{22}^2\xi_f. \quad (26)$$

where y_f and ξ_f are fast parts of the corresponding variable in (22). The fast dynamics (26) in original time-scale t is

$$\dot{\xi}_f(t) = (I_{n-m} \otimes A)\xi_f(t) + (I_{n-m} \otimes B)u_f(t), \quad (27)$$

where $u_f(t) = -K_{n-m}^{int}(\Lambda^{int} \otimes I_{n_x})\xi_f(t)$.

The fast dynamics (27) corresponds to the intra-cluster dynamics, and hence the dynamics are dominated by the internal gain and the eigenvalues of the intra-cluster Laplacian. With the suitable choice of the internal gain K_k^{int} , the system (27) is exponentially stable.

Remark 3 We note that the stabilization of the synchronization error dynamics, i.e., the stabilization of dynamics ξ implies the synchronization inside the cluster.

Note that we use slow (t_s) and fast (t_f) time-scales for the analysis while the original time-scale (t) for the control design. This is possible because the transformations are invertible, and it can be verified by the definition of t_f and t_s .

3.5 Singular Perturbation Approximation

Now, we provide an approximation of the original system by the reduced-order subsystems in the following theorem. The proof follows from Theorem 5.1, [19]. But before stating the result, we make the following assumption on the existence of the control gains.

Assumption 3 *There exists an internal gain K^{int} and an external gain K^{ext} such that the slow dynamics (25) is synchronized and the fast dynamics (27) is stabilized.*

Remark 4 *Although we assume the existence of the synchronizing internal and external gain, it will be ensured by design in the next section that such gains exist.*

Theorem 1 *Let K^{ext} be designed such that $\|A\| \leq c_1 \mu^{ext}$ with $c_1 > 0$ and under Assumption 3, if $\text{Re } \lambda(A_{22}^2) < 0$, there exists a $\epsilon^* > 0$ such that, for all $\epsilon \in (0, \epsilon^*]$, the original system (22) starting from any bounded initial conditions y_0 and ξ_0 , is approximated for all finite time $t \geq t_0$ by*

$$\begin{cases} y = y_s(t_s) + \mathcal{O}(\epsilon) \\ \xi = \xi_f(t_f) + \mathcal{O}(\epsilon), \end{cases} \quad (28)$$

where $y_s \in \mathbb{R}^{m \cdot n_x}$ and $\xi_f \in \mathbb{R}^{(n-m) \cdot n_x}$ are the respective slow and the fast variables.

PROOF. See Appendix. ■

In the next section, we present the control design strategy i.e., the design of gains K^{int} and K^{ext} , to stabilize the fast subsystems and synchronize the slow subsystems, respectively.

4 Control Design Scheme

In this section, we present a controller design strategy for system (19). Using the idea of timescale separation, we split the design procedure into two parts corresponding to the internal and the external control.

First, based on the fast dynamics (27) we design an internal control using the local information that ensures the synchronization inside the cluster. Then, we use the slow dynamics (25) for the design of external control to achieve synchronization between the clusters. While the internal controller is optimal, the external control is designed to ensure the cost is below a given threshold. Finally, Theorem 1 is used to justify such a separation of the system analysis in two steps and to approximate overall network behavior in terms of fast and slow dynamics.

In what follows, we first address the internal control design and give an analytical gain expression for the case of a complete graph inside clusters. The fast dynamics obtained after the time-scale separation represent the synchronization dynamics of an isolated cluster. Under assumption 2, this

dynamics can be further decoupled into subsystems corresponding to each agent.

4.1 Internal (Fast) Control Design

As the fast variable ξ_f is an approximation of the synchronization error ξ inside the clusters, it is still relevant to consider the fast subsystems (27) for the internal control design. We denote by $\xi_{f,k} \in \mathbb{R}^{(n_k-1) \cdot n_x}$ the component of $\xi_f := (\xi_{f,1}, \dots, \xi_{f,m})$ corresponding to the k -th cluster. For each cluster \mathcal{C}_k , for $k \in \mathcal{M}$, we have the following dynamics

$$\begin{cases} \dot{\xi}_{f,k}(t) = (I_{n_k-1} \otimes A)\xi_{f,k}(t) + (I_{n_k-1} \otimes B)u_{f,k}(t), \\ u_{f,k}(t) = -(\Lambda_k^{int} \otimes K_k^{int})\xi_{f,k}(t). \end{cases} \quad (29)$$

The cluster cost associated with the cluster \mathcal{C}_k takes the form

$$J_{f,k} = \int_0^{+\infty} \xi_{f,k}^\top (\Lambda_k^{int} \otimes I_{n_x}) \xi_{f,k} + u_{f,k}^\top (I_{n_k-1} \otimes R_k) u_{f,k} dt. \quad (30)$$

Instead of considering the internal cluster cost (8), we approximate the internal cost by the cost function (30) and the validity of the approximation is justified in the Theorem 2.

Recall that under Assumption 2, the eigenvalues of the internal Laplacian of the dense clusters are approximated by n_k for each $k \in \mathcal{M}$ i.e., $\Lambda_k^{int} = n_k I_{n_k-1}$ for each $k \in \mathcal{M}$. Thus, the matrices in equations (29) and (30) have block-diagonal form and they can be decoupled into $n_k - 1$ independent subsystems. For each cluster \mathcal{C}_k , similarly to ξ_k defined in equation (13), let us denote the fast subsystems and the associated control by $\xi_{f,k,i} := (\xi_{f,k,1}, \dots, \xi_{f,k,n_k-1})$ and $u_{f,k,i} := (u_{f,k,1}, \dots, u_{f,k,n_k-1})$, respectively. Then, for $i = 1, \dots, n_k - 1$ and for all $k \in \mathcal{M}$, the dynamics are

$$\begin{cases} \dot{\xi}_{f,k,i}(t) = A\xi_{f,k,i}(t) + n_k B u_{f,k,i}(t), \\ u_{f,k,i}(t) = -K_k^{int} \xi_{f,k,i}(t), \end{cases} \quad (31)$$

and the associated individual cost is

$$J_{f,k,i} = \int_0^{+\infty} n_k \xi_{f,k,i}^\top \xi_{f,k,i} + n_k^2 u_{f,k,i}^\top R_k u_{f,k,i} dt. \quad (32)$$

Thus, the cost (30) can be expressed as the sum of individual costs (32) as follows, $J_{f,k} = \sum_{i=1}^{n_k-1} J_{f,k,i}$, $\forall k \in \mathcal{M}$.

Remark 5 *The decoupling of dynamics (29) into $n_k - 1$ subsystems (31) is not only limited to the condition in Assumption 2. In the case, where we know the eigenvalues of the Laplacian or the Laplacian eigenvalues can be characterized in terms of n_k (for example, star graph), similar decoupling can be achieved.*

Remark 6 *It is noteworthy that the gain K_k^{int} is the same for all the agents belonging to the same cluster \mathcal{C}_k . As a*

result, the rewriting of (30) as a sum of individual cost (32) reduces the computational effort for the control design. Indeed, one can solve only one optimization problem (31)-(32) for each cluster and it is equivalent to optimizing the cluster cost (30).

Next, we show that the system (31) is stabilizable with a simple linear controller, while we recall that the system (31) corresponds to fast dynamics of our original system. Finally, we apply the LQ-control [18] to stabilize (31) while minimizing the cost (32).

Lemma 2 Consider the system (31), under assumption 1, if the pair (A, B) is stabilizable and $(A, (R_k)^{1/2})$ is detectable, then for every $k \in \mathcal{M}$, the system (31) is stabilizable while minimizing the cost (32) by a controller $u_{f,k,i}(t) = -K_k^{int} \xi_{f,k,i}(t)$ with the gain

$$K_k^{int} = \frac{R_k^{-1}}{n_k} B^\top P_k^{int}, \quad k \in \mathcal{M}, \quad (33)$$

where P_k^{int} is the solution of the Algebraic Riccati Equation (ARE)

$$P_k^{int} A + A^\top P_k^{int} - P_k^{int} B R_k^{-1} B^\top P_k^{int} + n_k I_{n_x} = 0. \quad (34)$$

From Lemma 2, we observe that the fast dynamics (31) is exponentially stable i.e., $\xi_f(t) \rightarrow 0$ as $t \rightarrow \infty$. And this implies synchronization inside the clusters, since, from equation (15) we have $e_k = Z_k^\top \xi_f + \mathcal{O}(\epsilon)$. Now, we pass to the design of the external controller.

4.2 External (Slow) Control Design

In this sub-section, we present the external controller design based on the slow dynamics (25). To achieve the synchronization between the clusters, we propose a method based on [31]. First, the synchronization problem is transformed into a stabilization problem using a change of variable. Then, we design the control to stabilize the system while upper-bounding the associated cost.

Recall that if the clusters are synchronized, the agents in each cluster behave like a single node, and the number of nodes representing the external network equals the number of clusters. Thus, the external graph of agents between clusters is only connected, and hence the standard optimization or the optimal control approaches cannot be applied directly. In this context, inspired by the notion in game theory, we use the satisfaction equilibrium approach, and satisfaction games [29]. A set of actions are said to be in satisfaction equilibrium when the individual cost for each agent is upper-bounded by a given threshold.

4.2.1 Average Dynamics

The slow dynamics obtained after time-scale separation in equation (25) defines the dynamics of the average of each

cluster. Following from equation (25), the average dynamics can be written as

$$\dot{y}_s(t) = ((I_m \otimes A) - (I_m \otimes B) \bar{K}^{ext} (\bar{\mathcal{L}}^{ext} \otimes I_{n_x})) y_s(t), \quad (35)$$

where $\bar{K}^{ext} = \text{diag}(K_1^{ext}, \dots, K_m^{ext})$ is the external gain and

$(\bar{\mathcal{L}}^{ext} \otimes I_{n_x}) = H(\mathcal{L}^{ext} \otimes I_{n_x}) \tilde{H}$ with the following form

$$\bar{\mathcal{L}}^{ext} = \begin{pmatrix} \sum_{l=2}^m \frac{a_{1l}^{ext}}{n_1} - \frac{a_{12}^{ext}}{n_1} & \dots & -\frac{a_{1m}^{ext}}{n_1} \\ \vdots & \ddots & \vdots \\ -\frac{a_{m1}^{ext}}{n_m} & -\frac{a_{m2}^{ext}}{n_m} & \dots & \sum_{l=1}^{m-1} \frac{a_{ml}^{ext}}{n_m} \end{pmatrix} \in \mathbb{R}^{m \times m},$$

is the average Laplacian matrix related to (35). In average Laplacian, $\bar{\mathcal{L}}^{ext}$ the diagonal elements represent the total number of external connections from a cluster $k \in \mathcal{M}$ to the rest of the network and the non-diagonal entries a_{kl}^{ext} represents the total number of connections between cluster \mathcal{C}_k and \mathcal{C}_l .

Let us denote by $y_{s,k} \in \mathbb{R}^{n_x}$ the k -th component of the variable y_s . Then, the average dynamics of each cluster \mathcal{C}_k , for $k \in \mathcal{M}$, based on equation (35) is

$$\begin{cases} \dot{y}_{s,k} = A y_{s,k} + B u_{s,k}^{ext}, \\ u_{s,k}^{ext} = -K_k^{ext} \sum_{l \in \mathcal{N}_{C_k}} \frac{a_{kl}^{ext}}{n_k} (y_{s,k} - y_{s,l}) \end{cases} \quad (36)$$

where, $u_{s,k}^{ext}$ can be viewed as the control on the cluster level, since it represents the sum of the individual controllers. For system (36) we define the average cost for each cluster $\mathcal{C}_k, k \in \mathcal{M}$, as

$$\bar{J}_k^{ext} = \int_0^{+\infty} \sum_{l \in \mathcal{N}_{C_k}} \frac{a_{kl}^{ext}}{n_k} (y_{s,k} - y_{s,l})^2 + n_k \sum_{i=1}^{n_k} \hat{u}_{k,i}^{ext \top} R_k \hat{u}_{k,i}^{ext} dt \quad (37)$$

where

$$\hat{u}_{k,i}^{ext} := -K_k^{ext} \sum_{l \in \mathcal{N}_{C_k}} \frac{a_{(k,i) \leftrightarrow C_l}^{ext}}{n_k} (y_{s,k} - y_{s,l}) \quad \forall i \in C_k, \quad (38)$$

and $a_{(k,i) \leftrightarrow C_l}^{ext}$ is the total number of connections between the i -th agent belonging to \mathcal{C}_k and the cluster \mathcal{C}_l and clearly $a_{(k,i) \leftrightarrow C_l}^{ext} \leq n_k$. The control $\hat{u}_{k,i}^{ext}$ is the external control (6) expressed in the average variable y_s . In addition, we have the relation $u_{s,k}^{ext} = \sum_{i=1}^{n_k} \hat{u}_{k,i}^{ext}$ and $a_{kl}^{ext} = \sum_{i=1}^{n_k} a_{(k,i) \leftrightarrow C_l}^{ext}$.

Notice that the average cost (37) is different from the external cost function that appears in equation (8) in several ways:

- the average variable $y_{s,k}$ is used instead of the original state variables x_k for each cluster, and

- although the clusters have merged into a single node, the agents still apply the individual control (6) rather than the average control (36). Thus, we express the individual external control (6) in average variables y_s in equation (38) and define the average cost (37) in terms of the original control. It is possible to define the cost function as a function of average control $u_{s,k}^{ext}$ as follows,

$$\bar{J}_k^{ext} = \int_0^{+\infty} \sum_{l \in \mathcal{N}_{C_k}} \frac{a_{kl}^{ext}}{n_k} (y_{s,k} - y_{s,l})^2 + u_{s,k}^{ext \top} R_k u_{s,k}^{ext} dt, \quad (39)$$

however, we remark that optimization of the average cost does not necessarily imply optimization of individual cost.

In the following, we perform the change of variables to design an external gain synchronizing the network of clusters.

4.2.2 Change of Variables

To study the consensus between the clusters, we define the external error variable for each cluster C_k . Let us define $Y_{k,l} = (y_{s,l} - y_{s,k}), l \neq k$. Then the external error variable for each cluster $C_k, k \in \mathcal{M}$ is defined as

$$Y_k := \left(Y_{k,1}^\top, \dots, Y_{k,k-1}^\top, Y_{k,k+1}^\top, \dots, Y_{k,m}^\top \right)^\top \in \mathbb{R}^{(m-1) \cdot n_x}. \quad (40)$$

Then, based on equation (40), the corresponding external error dynamics is

$$\dot{Y}_k = \mathbf{A}_k Y_k + \mathbf{B}_k u_{s,k}^{ext}, \quad \forall k \in \mathcal{M},$$

where,

$$\begin{aligned} \mathbf{A}_k &= (I_{m-1} \otimes A) - (I_{m-1} \otimes B) \bar{K}_{-k}^{ext} (\bar{\mathcal{L}}_{-k}^{ext} \otimes I_{n_x}), \\ \mathbf{B}_k &= -(I_{m-1} \otimes B). \end{aligned} \quad (41)$$

Here, $\bar{K}_{-k}^{ext} = \text{diag}(K_1^{ext}, \dots, K_{k-1}^{ext}, K_{k+1}^{ext}, \dots, K_m^{ext})$ is not a control action, but it represents the behavior of the network.

To recast the average cost function (37) in terms of new variables Y_k , we introduce the following notations. First we look into the structure of the external Laplacian which have the block form as follows,

$$\mathcal{L}^{ext} = \begin{pmatrix} \mathcal{L}_{1,1}^{ext} & \mathcal{L}_{1,2}^{ext} & \dots & \mathcal{L}_{1,m}^{ext} \\ \mathcal{L}_{2,1}^{ext} & \mathcal{L}_{2,2}^{ext} & \dots & \mathcal{L}_{2,m}^{ext} \\ \vdots & \vdots & & \vdots \\ \mathcal{L}_{m,1}^{ext} & \mathcal{L}_{m,2}^{ext} & \dots & \mathcal{L}_{m,m}^{ext} \end{pmatrix} \in \mathbb{R}^{n \times n}, \quad (42)$$

where $\mathcal{L}_{p,q}^{ext} \in \mathbb{R}^{n_p \times n_q}$ for $p, q \in \mathcal{M}$. We denote by $\mathcal{L}_{k,row}^{ext} \in \mathbb{R}^{n_k \times n}$ the k -th row of the block-matrix (42) for all $k \in \mathcal{M}$. It describes the connections of the cluster C_k with the rest of the agents in the network. The matrix $\mathcal{L}_{k,red}^{ext} \in \mathbb{R}^{n_k \times (n-n_k)}$ is obtained by removing the $\mathcal{L}_{k,k}^{ext}$ block from the $\mathcal{L}_{k,row}^{ext}$.

For example, $\mathcal{L}_{2,row}^{ext} = [\mathcal{L}_{2,1}^{ext} \ \mathcal{L}_{2,2}^{ext} \ \dots \ \mathcal{L}_{2,m}^{ext}]$ and $\mathcal{L}_{2,red}^{ext} = [\mathcal{L}_{2,1}^{ext} \ \mathcal{L}_{2,3}^{ext} \ \dots \ \mathcal{L}_{2,m}^{ext}]$. Then, we rewrite the external cost (37) in terms of new variables as

$$\bar{J}_k^{ext} = \int_0^{+\infty} Y_k^\top Q_{k,1}^{ext} Y_k + Y_k^\top \frac{Q_{k,2}^{ext}}{n_k} Y_k dt \quad (43)$$

where

$$\begin{aligned} Q_{k,1}^{ext} &= \left(\text{diag} \left(\frac{a_{k,1}^{ext}}{n_k}, \dots, \frac{a_{k,k-1}^{ext}}{n_k}, \frac{a_{k,k+1}^{ext}}{n_k}, \dots, \frac{a_{k,m}^{ext}}{n_k} \right) \otimes I_{n_x} \right), \\ Q_{k,2}^{ext} &= U_{-k}^\top (\mathcal{L}_{k,red}^{ext \top} \mathcal{L}_{k,red}^{ext} \otimes K_k^{ext \top} R_k K_k^{ext}) U_{-k}, \\ U &= (\text{diag}(\mathbb{1}_{n_1}, \dots, \mathbb{1}_{n_m}) \otimes I_{n_x}), \\ R_k &> 0. \end{aligned} \quad (44)$$

The matrices $Q_{k,1}^{ext}$ and $Q_{k,2}^{ext}$ simplify the expressions in (37) such that $Y_k^\top Q_{k,1}^{ext} Y_k = \sum_{l \in \mathcal{N}_{C_k}} \frac{a_{kl}^{ext}}{n_k} (y_{s,k} - y_{s,l})^2$ and

$$Y_k^\top \frac{Q_{k,2}^{ext}}{n_k} Y_k = n_k \sum_{i=1}^{n_k} \hat{u}_{k,i}^{ext \top} R_k \hat{u}_{k,i}^{ext}.$$

4.2.3 Control Design

We will use the error dynamics (41) to design the external gain profile using the satisfaction equilibrium approach. It characterizes the external gain profile synchronizing the network in such a way that each cost (37) is bounded, i.e.,

$$\bar{J}_k^{ext} \leq \gamma^{ext} \|Y_k(0)\|^2, \quad \text{for } k \in \mathcal{M}. \quad (45)$$

The term $\|Y_k(0)\|$ represents the initial condition of the cluster C_k while γ^{ext} is a given threshold. In particular, the following proposition is valid.

Proposition 1 (Prop 1, [31]) *Let a gain profile $\bar{K}^{ext} = \text{diag}(K_1^{ext}, \dots, K_m^{ext})$ be given. The following statements are equivalent,*

- (1) *The gain profile \bar{K}^{ext} is an SE of the satisfaction game (41) for all $k \in \mathcal{M}$.*
- (2) *For all $k \in \mathcal{M}$, there exists a positive-definite matrix $P_k^{ext} > 0$ such that*

$$\begin{cases} P_k^{ext} \mathbf{A}_{k,cl}(K_k^{ext}) + \mathbf{A}_{k,cl}^\top(K_k^{ext}) P_k^{ext} + \mathbf{Q}_k^{ext}(K_k^{ext}) < 0, \\ P_k^{ext} - \gamma^{ext} I_{(m-1) \cdot n_x} < 0, \end{cases} \quad (46)$$

where

$$\begin{cases} \mathbf{A}_{k,cl}(K_k^{ext}) = \mathbf{A}_k + \mathbf{B}_k K_k^{ext} (F_k \otimes I_{n_x}), \\ F_k = \left(\frac{a_{k,1}^{ext}}{n_k}, \dots, \frac{a_{k,k-1}^{ext}}{n_k}, \frac{a_{k,k+1}^{ext}}{n_k}, \dots, \frac{a_{k,m}^{ext}}{n_k} \right), \\ \mathbf{Q}_k^{ext} = \left(Q_{k,1}^{ext} + \frac{Q_{k,2}^{ext}}{n_k} \right). \end{cases} \quad (47)$$

Next, we present the algorithm that allows us to obtain the gain (K^{ext}) in satisfaction equilibrium. This algorithm greatly reduces the computational effort of obtaining the synchronizing gain for large-scale networks.

4.3 Algorithm

Consider a network of m clusters (the number of clusters in our case) with their respective dynamics. We aim to design a synchronizing gain profile $K^{ext} = (K_1^{ext}, \dots, K_m^{ext})$ satisfying the cost constraints.

In the following algorithm, we first calculate the internal gain by solving the algebraic Riccati equation (34). To design the external gain (K^{ext}), we start with the initial gain profile that satisfies the LMI (46). Then we multiply the gain from the previous iteration with a scalar $\alpha^{ext} \in \mathbb{R}_+ \setminus \{0\}$ and check if it satisfies the LMI (46), to obtain the sub-optimal gain. One approach could be to start with a high gain and decrease α^{ext} until the condition (46) is not satisfied and use the smallest gain that satisfied the condition.

Furthermore, we should also make sure the network parameter ϵ is small so that the control design using time-scale separation holds. Thus, to ensure this, we multiply the internal gain K_k^{int} with ϵ/ϵ^* to obtain the new internal gain such that $\epsilon \leq \epsilon^*$.

Algorithm 1 Sequential Satisfaction Algorithm

Data: A, B and $n_k, k \in \mathcal{M}$;
Set: iterations $itr = 1$, maximum number of iterations itr_{max} , $0 < \epsilon^* \ll 1$ and $K^{ext}(0) = (K_1^{ext}(0), \dots, K_m^{ext}(0))$ initial gain profile synchronizing the system ;
Calculate: P_k^{int} and K_k^{int} using equation (34) and (33) for all $k \in \mathcal{M}$, respectively;
while LMIs (46) not satisfied **OR** $itr \leq itr_{max}$ **do**
 $K^{ext}(itr + 1) \leftarrow \alpha^{ext} K^{ext}(itr)$, $\alpha^{ext} \in \mathbb{R}_+ \setminus \{0\}$;
 Calculate: ϵ ;
 if $\epsilon > \epsilon^*$ **then**
 $K_k^{int}(itr + 1) \leftarrow \frac{\epsilon}{\epsilon^*} K_k^{int}(itr)$;
 else
 $K_k^{int}(itr + 1) \leftarrow K_k^{int}(itr)$;
 end if
end while

Remark 7 Notice that with such an approach, we only scale the whole matrix K_k^{int} and K_k^{ext} on each step while keeping the structure of the matrix intact.

In the algorithm 1, to obtain the initial gain profile $K^{ext}(0)$ we use the algorithm in [3] which has the computational complexity of $\mathcal{O}(m)$ for m clusters. Then, the computational complexity to obtain the internal gain is of order $\mathcal{O}(m)$. Notice that the dimension of the matrix P_k^{int} in equation (34) does not depend on the number of agents (n_k) in the cluster, thus the problem of finding the internal control K_k^{int}

is independent of the number of agents in the cluster. To obtain the external gain, K^{ext} we use the SeDuMi [20]. The computational complexity of verifying, if the gain profile satisfies the LMI condition (50) using SeDuMi is $\mathcal{O}(m^{5.5})$. Thus, the overall computational complexity of the Algorithm 1 is $\mathcal{O}(m) + \mathcal{O}(m) + \mathcal{O}(m^{5.5})$. Moreover, from Lemma 2 we obtain the stabilizing internal gain K^{int} and if the algorithm successfully converges to synchronizing external gain (K^{ext}) that satisfies LMI conditions (46), then they will satisfy the Assumption 3.

5 Global System Analysis

In this section, we analyze the overall networked system with the controller gains K^{int} and K^{ext} defined by the Algorithm 1 and designed for reduced slow and fast subsystems. First, we present the proposition which ensures that the slow and fast controllers, designed independently of each other, synchronize the overall network. And finally, we prove that the cluster cost $J_k(T, +\infty)$ is approximated only by the external cost $J_k^{ext}(T, +\infty)$, where $T > 0$ is a finite time at which each cluster has reached internal synchronization.

5.1 Overall Network Behavior

Based on the controller design procedure presented in the section 4, we ensure that the Assumption 3 is satisfied i.e., the internal gain stabilizing the fast dynamics and the external gain synchronizing the slow dynamics exist. Note that the presented design strategy optimizes the cost function (30) associated with the internal controller and upper bound the cost function (37) corresponding to the external controller. Hence, the obtained internal control gain is optimal while the external control gain is sub-optimal. Now, we apply these gains to achieve synchronization in the overall network, and the following proposition ensures synchronization.

Proposition 2 Consider the closed-loop network dynamics (18) and let the internal and external control gains be chosen based on Lemma 2 and Proposition 1, then the overall network synchronizes and satisfies the following bounds,

$$\begin{aligned} y(t) &= y_s(t) + \mathcal{O}(\epsilon) \\ \xi(t) &= \xi_f(\mu^{int}t) + \mathcal{O}(\epsilon). \end{aligned} \quad (48)$$

PROOF. The proof follows from Theorem 2. ■

5.2 Cost Approximation

In this subsection, we prove that the cluster cost can be approximated by the average cost after finite time T . The motivation is derived from the fact that the internal dynamics converge rapidly to the consensus, and external dynamics exhibit the dominating network behavior. We prove that for the time $t \in [T, +\infty)$, the cluster cost J_k is approximated by n_k times the average external cost, i.e., $n_k \bar{J}_k^{ext}$.

To provide this approximation result, we first define the internal error bound, which helps us characterize the time $T > 0$. And secondly, we ensure that the exponential stability of the fast dynamics (27) implies the exponential stability of the error dynamics (19).

The necessity of the internal error bound arises in the approximation of the cluster cost. During the control design, we recall that the internal consensus is considered to be achieved before designing the external control. Thus, we need to characterize an error bound for the internal cost in finite time T , at which the cluster is very close to the internal consensus. More precisely, the bound at the time $T > 0$ such that $|\xi_{f,k}(T)| \leq \epsilon$ for all $k \in \mathcal{M}$.

The closed-loop fast dynamics is

$$\dot{\xi}_{f,k}(t) = ((I_{n_k-1} \otimes A) - (\Lambda_k^{int} \otimes BK_k^{int}))\xi_{f,k}(t),$$

and

$$\xi_{f,k}(t) = e^{Cl_{f,k}t}\xi_{f,k}(0),$$

where $Cl_{f,k} := ((I_{n_k-1} \otimes A) - (\Lambda_k^{int} \otimes BK_k^{int}))$ and $Cl_{f,k} < 0$ due to Lemma 2. Now, taking norm on both sides and from the definition of the measure of the matrix (see notations and preliminaries for definition), we obtain,

$$\|\xi_{f,k}(t)\| = e^{\nu(Cl_{f,k})t}\|\xi_{f,k}(0)\| \leq e^{\nu(Cl_f)t}\|\xi_{f,k}(0)\|$$

where $\nu(Cl_f) = \max_{k \in \mathcal{M}} \nu(Cl_{f,k})$. Then, as an internal error bound, we choose smallest $T \geq 0$ such that

$$\|\xi_{f,k}(T)\| \leq e^{\nu(Cl_f)T} \max_{k \in \mathcal{M}} \|\xi_{f,k}(0)\| \leq \epsilon.$$

This bound characterizes the local consensus inside each cluster in the finite time T . And hence, it yields

$$\|\xi_{f,k}(t)\| \leq \epsilon e^{\nu(Cl_f)(t-T)} \quad \forall k \in \mathcal{M},$$

and

$$\|\xi_f(t)\| \leq \epsilon \sqrt{n-m} e^{\nu(Cl_f)(t-T)}. \quad (49)$$

Next, in equation (28), we notice that the approximation of ξ defined in equation (19) depends on the fast variable ξ_f and the slow variable y_s , but the slow variable may or may not be stable. For the network to achieve synchronization, ξ should be stable. Thus, we prove the following lemma, which ensures the exponential stability of ξ provided that ξ_f is exponentially stable.

Lemma 3 *The exponential stability of the fast dynamics (27) and the external error dynamics (41) implies the exponential stability of the error dynamics in (19).*

PROOF. See Appendix. ■

Next, with error bound for a finite time, T we present the cluster cost approximation for $t \in [T, +\infty)$. The proposition is stated as follows:

Proposition 3 *During the time interval $[T, +\infty)$, the following approximation holds,*

$$J_k(T, +\infty) = n_k \bar{J}_k^{ext}(T, +\infty) + \mathcal{O}(\epsilon), \quad \forall k \in \mathcal{M}. \quad (50)$$

PROOF. See Appendix. ■

Finally, we present the following theorem that bounds the total cluster cost with the sum of internal, external and the constant term.

Theorem 2 *The total cluster cost for all clusters \mathcal{C}_k , $k \in \mathcal{M}$ satisfy the following bound:*

$$J_k \leq (\|P_k^{int}\| + n_k \gamma_k + \mathbf{C}_k) \|x(0)\|^2 + \mathcal{O}(\epsilon) \quad (51)$$

where P_k^{int} is the solution of the Riccati equation (34) and \mathbf{C}_k is a constant.

PROOF. See Appendix. ■

6 Simulation

This section provides numerical results to illustrate the effectiveness of the control procedure and the cost approximation using three scenarios. The agent's dynamics are given by (1), where

$$A = \begin{pmatrix} 0.15 & 0.98 \\ -0.98 & 0.15 \end{pmatrix}, B = \begin{pmatrix} 1 \\ 1 \end{pmatrix}. \quad (52)$$

The external graph between the agents in different clusters is generated using Erdos-Renyi [14] random graph generator. Then the internal graph with all-to-all connections for each cluster is generated and added to the external graph to obtain the network graph. For the numerical illustration, we consider the multiple scenarios.

- **Scenario 1:** Graph \mathcal{G}_1 with 4 clusters with 630 agents. The clusters are labeled $\mathcal{C}_1, \dots, \mathcal{C}_4$ and number of agents in each cluster are given in Table 2. Each cluster has **all-to-all** internal connections and 299 external connections between the clusters in total. The threshold for the external cost is $\gamma^{ext} = 0.8$.
- **Scenario 2:** Same as Scenario 1 with **dense** internal connections instead of all-to-all internal connections.
- **Scenario 3:** Comparison of control design presented in this paper with the satisfactory control approach in [31] and guaranteed cost approach proposed in [3].

The details of the simulations are present in Tables 2 - 5. In the tables, n_k represent the number of agents in cluster \mathcal{C}_k , $E_k = \frac{|J_k - n_k \bar{J}_k^{ext}|}{J_k} \times 100$, is the error percentage between the total cost and the external cost after time T , and K^{ext} and K^{int} are the respective external and internal gains.

6.1 Scenario 1: All-to-all connections in Clusters

In this scenario, we consider complete clusters and the values of the internal & external gains and the parameter ϵ calculated using the Algorithm 1, are presented in Table 1. The network \mathcal{G}_1 synchronizes upon applying these gains and it is shown in Figure 2. We can observe the four branches appearing and merging into one and each branch represents the local agreement within the clusters. Next, Figure 3 illustrates the cost approximation for the cluster \mathcal{C}_4 by comparing the total cluster cost J_4 and the external cost $n_4 \bar{J}_4^{ext}$, after finite time $T = 2s$.

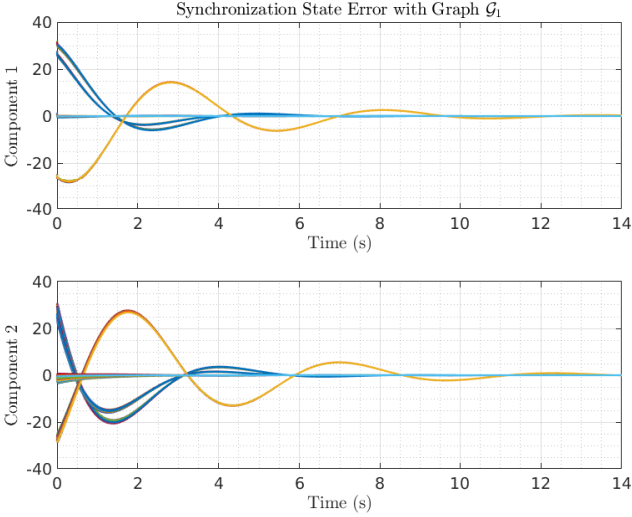


Fig. 2. Evolution of the error between the agents' state in graph \mathcal{G}_1 with all-to-all connections inside clusters.

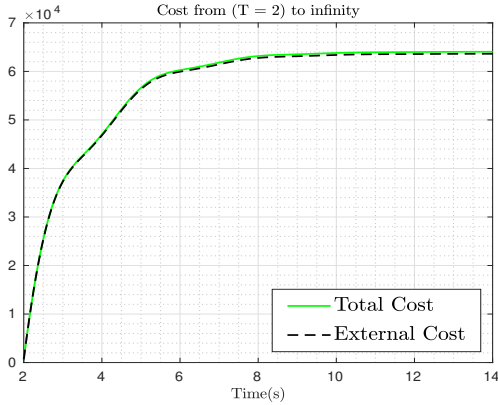


Fig. 3. Evolution of the costs J_4 and $n_4 \bar{J}_4^{ext}$ with all-to-all connections inside clusters.

6.2 Scenario 2: Connected Clusters

In this scenario, we consider the graph (\mathcal{G}_2) where the clusters have dense interconnections. The graph for each cluster in the graph (\mathcal{G}_2) is generated using ErdosRenyi [14] random graph generator with the average number of connections for each agent in the respective cluster denoted by \mathcal{C}_{avg}

Clusters	K^{int}	K^{ext}
\mathcal{C}_1	[1.5352, -0.1102]	[0.85, 0.16]
\mathcal{C}_2	[1.5349, -0.1114]	[1.17, 0.22]
\mathcal{C}_3	[1.5346, -0.1128]	[0.59, 0.11]
\mathcal{C}_4	[1.5344, -0.1137]	[1.05, 0.2]

Table 1
Internal and External gains due to Algorithm 1.

$\epsilon = 0.06, \gamma^{ext} = 0.8$			
	n_k	$J_k (\times 10^5)$	E_k
\mathcal{C}_1	120	0.8966	0.45%
\mathcal{C}_2	140	0.5768	0.86%
\mathcal{C}_3	170	1.8950	0.24%
\mathcal{C}_4	200	0.6405	0.65%

Table 2
Simulation results for the network with complete (all-to-all) connections inside each cluster.

in Table 3. However, the number of agents and the number of external connections remain the same as in the graph \mathcal{G}_1 . The same gains from Scenario 1 (Table 1) are applied to the network system with the graph \mathcal{G}_2 . The cost associated with the gain in Table 1 is presented in Table 3. We can see that due to the change in the network structure (Scenario 2), the synchronization cost has changed as shown in Table 3.

	n_k	\mathcal{C}_{avg}	$J_k (\times 10^5)$	E_k
\mathcal{C}_1	120	96	0.8983	0.64%
\mathcal{C}_2	140	115	0.5780	1.07%
\mathcal{C}_3	170	145	1.8975	0.37%
\mathcal{C}_4	200	174	0.6415	0.81%

Table 3
Simulation results for the network with connected clusters.

6.3 Scenario 3

In the last scenario, we consider a network of $m = 4$ clusters with $n_k = 10$ agents in each. We recall that $\gamma^{ext} = 0.8$ is chosen for both controls. A comparison is made between the composite control proposed in this paper and the satisfactory control approach proposed in [31]. The design procedure in [31] needs 13752 seconds (3.8 hours) to compute the gains for $n = 40$ agents, while the composite design in this paper requires 13 seconds. However, we can observe an incontestable difference in performance on the cluster costs due to satisfactory control, as shown in table 4.

Next, we present a comparison with the algorithm in [3] that designs an identical control gain for all the agents, independently of the graph and aims to bound a global cost. Consequently the computational burden of the composite control is $\mathcal{O}(m)$ times the computational burden of the algorithm in [3]. Although the comparison of the the algorithm in [3] with the composite control is not fair since they apply in

	C_1	C_2	C_3	C_4
n_k	10	10	10	10
J_k	17204	5452	6943	16949
J_k^*	10164	3303	3080	9714

Table 4
Comparison of cost with the satisfactory control algorithm in [31].

different setups we give here a few elements. For a network of 630 nodes and 4 clusters the computational time due to the algorithm in [3] and the composite control in this paper are 0.3 and 33 seconds, respectively and the cost associated are present in Table 5. It shows that increased computational effort results in much better costs. On the other hand, the algorithm in [31] proposes the design of different control gains for every single agent, but the computational burden is much higher than the one required for our composite control. Basically, the computational effort is multiplied with n/m in [31] with respect to the composite control ones. We conclude that taking advantage of the clustered structure of the network leads to a good trade-off between the computational complexity and the closed-loop performances.

	C_1	C_2	C_3	C_4
n_k	120	140	170	200
$J_k (\times 10^6)$	0.385	0.269	0.689	0.262
$J_k^* (\times 10^6)$	6.7	8.1	16.7	20.5

Table 5
Comparison of the cost with the same gain algorithm in [3].

7 Conclusion

In this paper, we propose a distributed composite control design strategy for the clustered network. Using a coordinate transformation, the network dynamics is transformed into standard singular perturbation form and decoupled into slow and fast dynamics using time-scale separation. This decoupling of the network dynamics also decouples the control into fast (internal) and slow (external). The internal control is responsible for intra-cluster synchronization, while the external synchronizes the network while satisfying the imposed cost criterion. This independent design greatly reduces the computational effort required to obtain the control. Finally, we show that the cluster cost is approximated only by the external cost after a short time period.

References

- [1] B. Adhikari, I-C. Morărescu, and E. Panteley. An emerging dynamics approach for synchronization of linear heterogeneous agents interconnected over switching topologies. *IEEE Control Systems Letters*, 5(1):43–48, 2021.
- [2] V. N. Belykh, I. V. Belykh, and M. Hasler. Hierarchy and stability of partially synchronous oscillations of diffusively coupled dynamical systems. *Phys. Rev. E*, 62:6332–6345, Nov 2000.
- [3] J. Ben Rejeb, I-C. Morărescu, and J. Daafouz. Guaranteed cost control design for synchronization in networks of linear singularly perturbed systems. In *2017 IEEE 56th Annual Conference on Decision and Control (CDC)*, pages 1602–1607, 2017.
- [4] J. Bleibel, M. Habiger, M. Lütje, F. Hirschmann, F. Roosen-Runge, T. Seydel, F. Zhang, F. Schreiber, and M. Oettel. Two time scales for self and collective diffusion near the critical point in a simple patchy model for proteins with floating bonds. *Soft Matter*, 14:8006–8016, 2018.
- [5] A. M. Boker, T. R. Nudell, and A. Chakraborty. On aggregate control of clustered consensus networks. In *2015 American Control Conference (ACC)*, pages 5527–5532, 2015.
- [6] F. Borrelli and T. Keviczky. Distributed lqr design for identical dynamically decoupled systems. *IEEE Transactions on Automatic Control*, 53(8):1901–1912, 2008.
- [7] R. L. Breiger, S. A. Boorman, and P. Arabie. An algorithm for clustering relational data with applications to social network analysis and comparison with multidimensional scaling. *Journal of Mathematical Psychology*, 12(3):328–383, 1975.
- [8] E. Bıyık and M. Arcak. Area aggregation and time-scale modeling for sparse nonlinear networks. *Systems & Control Letters*, 57(2):142–149, 2008.
- [9] J. Chow and P. Kokotovic. A decomposition of near-optimum regulators for systems with slow and fast modes. *IEEE Transactions on Automatic Control*, 21(5):701–705, 1976.
- [10] J. Chow and P. Kokotovic. Time scale modeling of sparse dynamic networks. *IEEE Transactions on Automatic Control*, 30(8):714–722, Aug 1985.
- [11] J. H. Chow, Ed. Time-scale modeling of dynamic networks with applications to power systems. *Lecture Notes in Control and Information Sciences*, 1982.
- [12] G. De Pasquale and M. E. Valcher. Consensus for clusters of agents with cooperative and antagonistic relationships. *Automatica*, 135:110002, 2022.
- [13] A. S. Dolby and T. C. Grubb Jr. Benefits to satellite members in mixed-species foraging groups: an experimental analysis. *Animal behaviour*, 56(2):501–509, 1998.
- [14] P. Erdos, A. Rényi, et al. On the evolution of random graphs. *Publ. Math. Inst. Hung. Acad. Sci*, 5(1):17–60, 1960.
- [15] S. Hata and H. Nakao. Localization of laplacian eigenvectors on random networks. *Scientific reports*, 7(1):1–11, 2017.
- [16] A. Heniche and I. Karnwa. Control loops selection to damp inter-area oscillations of electrical networks. *IEEE Transactions on Power Systems*, 17(2):378–384, 2002.
- [17] H. Jaleel and J. S. Shamma. Decentralized energy aware co-optimization of mobility and communication in multiagent systems. In *2016 IEEE 55th Conference on Decision and Control (CDC)*, pages 2665–2670, 2016.

- [18] R. E. Kalman et al. Contributions to the theory of optimal control. *Bol. Soc. Mat. Mexicana*, 5(2):102–119, 1960.
- [19] P. Kokotović, H. K. Khalil, and J. O’Reilly. *Singular Perturbation Methods in Control: Analysis and Design*. Society for Industrial and Applied Mathematics, 1999.
- [20] Y. Labit, D. Peaucelle, and D. Henrion. Sedumi interface 1.02: a tool for solving lmi problems with sedumi. In *Proceedings. IEEE International Symposium on Computer Aided Control System Design*, pages 272–277. IEEE, 2002.
- [21] A. J. Laub. *Matrix analysis for scientists and engineers*, volume 91. Siam, 2005.
- [22] W. Lu, B. Liu, and T. Chen. Cluster synchronization in networks of coupled nonidentical dynamical systems. *Chaos*, 20 1:013120, 2010.
- [23] M. Maghenem, E. Panteley, and A. Loria. Singular-perturbations-based analysis of synchronization in heterogeneous networks: A case-study. In *2016 IEEE 55th Conference on Decision and Control (CDC)*, pages 2581–2586. IEEE, 2016.
- [24] S. Martin, I-C. Morărescu, and D. Nesic. Time scale modeling for consensus in sparse directed networks with time-varying topologies. *2016 IEEE 55th Conference on Decision and Control (CDC)*, Dec 2016.
- [25] J. Mytum-Smithson. Wireless sensor networks: An information processing approach. *Sensor Review*, 25(2), Jun 2005.
- [26] E. Panteley and A. Loria. Synchronization and dynamic consensus of heterogeneous networked systems. *IEEE Transactions on Automatic Control*, 62(8):3758–3773, 2017.
- [27] T. V. Pham, T. T. Doan, and D. H. Nguyen. Distributed two-time-scale methods over clustered networks. In *2021 American Control Conference (ACC)*, pages 4625–4630, 2021.
- [28] D. Romeres, F. Dörfler, and F. Bullo. Novel results on slow coherency in consensus and power networks. In *2013 European Control Conference (ECC)*, pages 742–747, 2013.
- [29] S. Ross and . Chaibdraa. Satisfaction equilibrium: Achieving cooperation in incomplete information games. In Luc Lamontagne and Mario Marchand, editors, *Advances in Artificial Intelligence*, pages 61–72, Berlin, Heidelberg, 2006. Springer Berlin Heidelberg.
- [30] E. Steur, I. Tyukin, A. Gorban, N. Jarman, H. Nijmeijer, and C. Leeuwen. Coupling-modulated multi-stability and coherent dynamics in directed networks of heterogeneous nonlinear oscillators with modular topology. *IFAC-PapersOnLine*, 49:62–67, 12 2016.
- [31] J. Veetaseveera, V. S. Varma, I-C. Morărescu, and J. Daafouz. Decentralized control for guaranteed individual costs in a linear multi-agent system: A satisfaction equilibrium approach. *IEEE Control Systems Letters*, 3(4):918–923, 2019.
- [32] S. Wasserman and K. Faust. *Social Network Analysis: Methods and Applications*. Structural Analysis in the Social Sciences. Cambridge University Press, 1994.

A Proofs

Proof of Lemma 1

We know from [21] $\|(A \otimes B)\| = \|A\|\|B\|$ for any matrix $A \in \mathbb{R}^{n \times n}$, $B \in \mathbb{R}^{m \times m}$. In addition, $\|H\| = \frac{1}{\sqrt{n}}$, $\|\tilde{H}\| = \sqrt{n}$ and $\|Z\| = \frac{1}{\sqrt{n}}$, $\|\tilde{Z}\| = \sqrt{n}$. It follows that,

$$\begin{aligned} \|\bar{A}_{11}\| &= \|(I_m \otimes A) - H(I_n \otimes B)K^{ext}(\mathcal{L}^{ext} \otimes I_{n_x})\tilde{H}\| \\ &\leq \|A\| + \|H\| \cdot \|(I_n \otimes B)K^{ext}(\mathcal{L}^{ext} \otimes I_{n_x})\| \cdot \|\tilde{H}\| \\ &= (c_1 + \sqrt{\frac{n}{n}})\mu^{ext} = c_2\mu^{ext} = c_2\epsilon\mu^{int}. \end{aligned} \quad (\text{A.1})$$

The bounds of \bar{A}_{12} , \bar{A}_{21} and \bar{A}_{22}^1 are derived similarly, that’s why we only prove for \bar{A}_{12} ,

$$\begin{aligned} \|\bar{A}_{12}\| &= \|H(I_n \otimes B)K^{ext}(\mathcal{L}^{ext} \otimes I_{n_x})\tilde{Z}\| \\ &\leq \sqrt{\frac{n}{n}}\mu^{ext} \leq c_2\mu^{ext} \leq c_2\epsilon\mu^{int}. \end{aligned} \quad (\text{A.2})$$

Then, we lower-bound the matrix \bar{A}_{22}^2 such that

$$\begin{aligned} \|\bar{A}_{22}^2\| &= \|(I_{n-m} \otimes A) - (I_{n-m} \otimes B)K_{n-m}^{int}(\Lambda^{int} \otimes I_{n_x})\| \\ &\geq \left| \|A\| - \|(I_{n-m} \otimes B)K_{n-m}^{int}(\Lambda^{int} \otimes I_{n_x})\| \right|. \end{aligned} \quad (\text{A.3})$$

From (21), we understand that the second term in (A.3) is much larger than the first one. Thus, by taking the difference between the largest value of the first term and the smallest value of the second term, it yields a lower-bound as

$$\|\bar{A}_{22}^2\| \geq |c_1\epsilon\mu^{int} - \mu^{int}| = |1 - c_1\epsilon|\mu^{int} \approx \mu^{int} \quad (\text{A.4})$$

since $\epsilon \ll 1$.

Proof of Theorem 1

The proof follows the reasoning in Theorem 5.1, Chapter 2, [19]. In [19], via similarity transformation, the authors express and decouple the original slow and fast variables into the approximated variables. The singularly perturbed system dynamics (22) is slightly different from the one in the [19]. Thus, we adapt the result from [19] to our system model to obtain the approximation results. The similarity transformations [19] for the decoupling of the dynamics (19) are

$$\begin{aligned} \begin{bmatrix} y \\ \xi \end{bmatrix} &= \begin{bmatrix} I_{m \cdot n_x} & \epsilon\Psi(\epsilon) \\ -\Omega(\epsilon) & I_{n_x(n-m)} - \epsilon\Omega(\epsilon)\Psi(\epsilon) \end{bmatrix} \begin{bmatrix} y_s \\ \xi_f \end{bmatrix} \\ \begin{bmatrix} y_s \\ \xi_f \end{bmatrix} &= \begin{bmatrix} I_{m \cdot n_x} - \epsilon\Psi(\epsilon)\Omega(\epsilon) & -\epsilon\Psi(\epsilon) \\ \Omega(\epsilon) & I_{n_x(n-m)} \end{bmatrix} \begin{bmatrix} y \\ \xi \end{bmatrix}, \end{aligned} \quad (\text{A.5})$$

where the functions Ω and Ψ should satisfy the following,

$$\begin{aligned} R(\Omega(\epsilon), \epsilon) &= \epsilon A_{21} - \epsilon A_{22}^1 \Omega(\epsilon) - A_{22}^2 \Omega(\epsilon) \\ &\quad + \epsilon \Omega(\epsilon) A_{11} - \epsilon \Omega(\epsilon) A_{12} \Omega(\epsilon) = 0, \\ S(\Psi(\epsilon), \epsilon) &= \epsilon A_{11} \Psi(\epsilon) + A_{12} - \epsilon A_{12} \Omega(\epsilon) \Psi(\epsilon) \\ &\quad - \epsilon \Psi(\epsilon) A_{22}^1 - \Psi(\epsilon) A_{22}^2 - \epsilon \Psi(\epsilon) \Omega(\epsilon) A_{12} = 0. \end{aligned}$$

The approximation of Ω and Ψ , obtained with the Taylor development w.r.t. ϵ , are

$$\begin{aligned}\Omega(\epsilon) &= \epsilon(A_{22}^2)^{-1}A_{21} + \mathcal{O}(\epsilon^2), \\ \Psi(\epsilon) &= A_{12}(A_{22}^2)^{-1} + \epsilon((A_{22}^2)^{-1}A_{11}A_{12}(A_{22}^2)^{-1} - A_{12}) \\ &\quad + \mathcal{O}(\epsilon^2).\end{aligned}\tag{A.6}$$

From Lemma (3), we know that $\xi(t)$ and $\xi_f(t_f)$ converge to zero exponentially as t and t_f tend to $+\infty$, respectively. Thus, we can claim that $\Omega(\epsilon)y_s(t)$ has an exponential decrease to zero w.r.t. t . Finally, from the above transformation (A.5), we have,

$$y = y_s(t_s) + \epsilon\Psi(\epsilon)\xi_f \tag{A.7}$$

$$\xi = \xi_f(t_f) - \Omega(\epsilon)y_s(t_s) - \epsilon\Omega(\epsilon)\Psi(\epsilon)\xi_f. \tag{A.8}$$

Then from (A.6), we have that $\Omega(\epsilon) = \mathcal{O}(\epsilon)$ and we obtain the approximations (28).

Proof of Lemma 3

Integrating the error dynamics in (19), we obtain

$$\begin{aligned}\xi(t) &= e^{\bar{A}_{22}t}\xi(0) + \int_0^t e^{\bar{A}_{22}(t-\tau)}\bar{A}_{21}y(\tau) d\tau \\ &= e^{\bar{A}_{22}t}\xi(0) + \int_0^t e^{\bar{A}_{22}(t-\tau)}\bar{A}_{21}(y_s(\tau) + \epsilon\Psi(\epsilon)\xi_f(\tau)) d\tau \\ &= e^{\bar{A}_{22}t}\xi(0) + \int_0^t e^{\bar{A}_{22}(t-\tau)}Z^TMY(\tau) d\tau \\ &\quad + \epsilon\int_0^t e^{\bar{A}_{22}(t-\tau)}\bar{A}_{21}\Psi(\epsilon)\xi_f(\tau) d\tau\end{aligned}$$

where $M = \text{diag}(M_1, \dots, M_m)$ and $M_k = (\mathcal{L}_{k,red}^{ext} \otimes BK_k^{ext})U_{-k}$. By taking norms on both sides, we have

$$\begin{aligned}\|\xi(t)\| &\leq \|e^{\bar{A}_{22}t}\|\|\xi(0)\| + \|Z^TM\|\int_0^t \|e^{\bar{A}_{22}(t-\tau)}\|\|Y(\tau)\| d\tau \\ &\quad + \epsilon\|\bar{A}_{21}\Psi(\epsilon)\|\int_0^t \|e^{\bar{A}_{22}(t-\tau)}\|\|\xi_f(\tau)\| d\tau\end{aligned}\tag{A.9}$$

Also, from the design of internal and external control, we know that, for all $t \geq 0$,

$$\begin{cases} Y(t) = e^{A_{cl}t}Y(0) \\ \xi_f(t) = e^{\bar{A}_{22}t}\xi_f(0) \end{cases} \Rightarrow \begin{cases} \|Y(t)\| \leq e^{\nu(A_{cl})t}\|Y(0)\| \\ \|\xi_f(t)\| \leq e^{\nu(\bar{A}_{22})t}\|\xi_f(0)\| \end{cases}\tag{A.10}$$

$A_{cl} = \text{diag}(A_{1,cl}, \dots, A_{m,cl})$ is the closed-loop dynamics of the external error (41). Then, it follows that

$$\begin{aligned}\|\xi(t)\| &\leq e^{\nu(\bar{A}_{22})t}\|\xi(0)\| \\ &\quad + \|Z^TM\|\|Y(0)\|\int_0^t e^{\nu(\bar{A}_{22})(t-\tau)}e^{\nu(A_{cl})\tau} d\tau \\ &\quad + \epsilon\|\bar{A}_{21}\Psi(\epsilon)\|\|\xi_f(0)\|\int_0^t e^{\nu(\bar{A}_{22})(t-\tau)}e^{\nu(\bar{A}_{22})\tau} d\tau.\end{aligned}$$

By integrating the second term in (A.9), we have

$$\begin{aligned}\|Z^TM\|\|Y(0)\|\int_0^t e^{\nu(\bar{A}_{22})(t-\tau)}e^{\nu(A_{cl})\tau} d\tau \\ = \|Z^TM\|\|Y(0)\|e^{\nu(\bar{A}_{22})t}\int_0^t e^{(\nu(A_{cl})-\nu(\bar{A}_{22}))\tau} d\tau \\ = \frac{\|Z^TM\|\|Y(0)\|}{\nu(A_{cl})-\nu(\bar{A}_{22})}\left[e^{\nu(A_{cl})t} - e^{\nu(\bar{A}_{22})t}\right].\end{aligned}$$

In the same manner, the third term is

$$\begin{aligned}\epsilon\|\bar{A}_{21}\Psi(\epsilon)\|\|\xi_f(0)\|\int_0^t e^{\nu(\bar{A}_{22})(t-\tau)}e^{\nu(\bar{A}_{22})\tau} d\tau \\ = \frac{\epsilon\|\bar{A}_{21}\Psi(\epsilon)\|\|\xi_f(0)\|}{\nu(\bar{A}_{22}^2) - \nu(\bar{A}_{22})}\left[e^{\nu(\bar{A}_{22}^2)t} - e^{\nu(\bar{A}_{22})t}\right].\end{aligned}\tag{A.11}$$

Finally, we have

$$\begin{aligned}\|\xi(t)\| &\leq \mathbf{C}_1 e^{\nu(A_{cl})t} + \epsilon\mathbf{C}_2 e^{\nu(\bar{A}_{22}^2)t} \\ &\quad + (\|\xi(0)\| - \mathbf{C}_1 - \epsilon\mathbf{C}_2) e^{\nu(\bar{A}_{22})t},\end{aligned}\tag{A.12}$$

where $\mathbf{C}_1 = \frac{\|Z^TM\|\|Y(0)\|}{\nu(A_{cl})-\nu(\bar{A}_{22})}$ and $\mathbf{C}_2 = \frac{\|\bar{A}_{21}\Psi(\epsilon)\|\|\xi_f(0)\|}{\nu(\bar{A}_{22}^2)-\nu(\bar{A}_{22})}$. Moreover, we know that $\nu(\bar{A}_{22}^2) < \nu(\bar{A}_{22}) < \nu(A_{cl}) < 0$. Thus, we conclude that ξ converges exponentially to zero and the rate of convergence can be bounded as

$$\|\xi(t)\| \leq \|\xi(0)\|e^{\nu(A_{cl})t}.\tag{A.13}$$

Proof of Proposition 3

The cost J_k is split into the sum of the internal and external costs and composite term, as shown in equation (8). Then, we bound the internal and external costs from time T to infinity. We proceed similarly with the composite term.

Internal Cost: Substituting $x_k = \tilde{H}_k y_k + \tilde{Z}_k \xi_k$ from equation (16) into J_k^{int} in equation (8) and with $\tilde{H}_k^\top (\mathcal{L}_k^{int} \otimes I_{n_x}) = 0$, it yields

$$\begin{aligned}J_k^{int}(T, +\infty) &= \int_T^{+\infty} \xi_k^\top \tilde{Z}_k ((\mathcal{L}_k^{int} \otimes I_{n_x}) \\ &\quad + (\mathcal{L}_k^{int\top} \mathcal{L}_k^{int} \otimes K_k^{int\top} R_k K_k^{int})) \tilde{Z}_k \xi_k dt, \\ &= \int_T^{+\infty} n_k \xi_k^\top \left((\Lambda_k^{int} \otimes I_{n_x}) \right. \\ &\quad \left. + \left(\Lambda_k^{int^2} \otimes P_k^{int\top} B \frac{R_k^{-1}}{n_k} B^\top P_k^{int} \right) \right) \xi_k dt, \\ &= \int_T^{+\infty} n_k \xi_k^\top ((\Lambda_k^{int} \otimes I_{n_x}) \\ &\quad + (I_{n_k-1} \otimes P_k^{int\top} B R_k^{-1} B^\top P_k^{int})) \xi_k dt, \\ &\leq \mathbf{C}_{3,k} \int_T^{+\infty} \|\xi_k\|^2 dt \leq \mathbf{C}_{3,k} \int_T^{+\infty} \|\xi(t)\|^2 dt.\end{aligned}$$

where

$\mathbf{C}_{3,k} = \|n_k((\Lambda_k^{int} \otimes I_{n_x}) + (I_{n_k-1} \otimes P_k^{int\top} B R_k^{-1} B^\top P_k^{int}))\|$. From Lemma 3 and equation (A.13), we have $\|\xi(t)\| \leq \|\xi(T)\|e^{\nu(A_{cl})(t-T)}$, for all $t \in [T, +\infty)$. Thus, with $\nu(A_{cl}) < 0$, we have,

$$\int_T^{+\infty} \|\xi(t)\|^2 dt \leq -\frac{\|\xi(T)\|^2}{2\nu(A_{cl})} = \mathbf{C}_4 \|\xi(T)\|^2 \tag{A.14}$$

where $\mathbf{C}_4 := (-\frac{1}{2\nu(A_{cl})})$. Thus, from (A.14)-(A.14) and the approximation of ξ in equation (28),

$$\begin{aligned}J_k^{int}(T, +\infty) &\leq \mathbf{C}_{3,k} \mathbf{C}_4 \|\xi_f(T) + \mathcal{O}(\epsilon)\|^2 \\ &\leq \mathbf{C}_{3,k} \mathbf{C}_4 (\|\xi_f(T)\|^2 + 2\mathcal{O}(\epsilon)\|\xi_f(T)\| + \mathcal{O}(\epsilon^2)).\end{aligned}$$

Finally, replacing $\|\xi_f(T)\| \leq \epsilon\sqrt{n-m}$ from (49) we have

$$J_k^{int}(T, +\infty) \leq \mathcal{O}(\epsilon^2).\tag{A.15}$$

External cost: First, we recast the collective external control (6) in the external error variable Y_k , as follows

$$\begin{aligned}u_k^{ext}(t) &= -(I_{n_k} \otimes K_k^{ext})(\mathcal{L}_{k,row}^{ext} \otimes I_{n_x})x(t) \\ &= -(\mathcal{L}_{k,row}^{ext} \otimes K_k^{ext})(\tilde{H}y(t) + \tilde{Z}\xi(t)) \\ &= -(\mathcal{L}_{k,row}^{ext} \otimes K_k^{ext})(\tilde{H}y_s(t) + \epsilon\tilde{H}\Psi(\epsilon)\xi_f(t_f) + \tilde{Z}\xi(t)) \\ &= (\mathcal{L}_{k,red}^{ext} \otimes K_k^{ext})U_{-k}Y_k(t) \\ &\quad - (\mathcal{L}_{k,row}^{ext} \otimes K_k^{ext})(\epsilon\tilde{H}\Psi(\epsilon)\xi_f(t_f) + \tilde{Z}\xi(t)),\end{aligned}\tag{A.16}$$

where $\mathcal{L}_{k,row}^{ext}$ is the k -th block-row of \mathcal{L}^{ext} and $\mathcal{L}_{k,red}^{ext}$ is obtained by removing the $\mathcal{L}_{k,k}^{ext}$ block from $\mathcal{L}_{k,row}^{ext}$. Then, it yields

$$\begin{aligned} & u_k^{ext \top}(t)(I_{n_k} \otimes R_k)u_k^{ext}(t) \\ &= Y_k^\top(t)Q_{k,2}^{ext}Y_k(t) + \epsilon^2 \xi_f^\top(t_f)D_{1,k}\xi_f(t_f) + \xi^\top(t)D_{2,k}\xi(t) \\ & - \epsilon Y_k^\top(t)D_{3,k}\xi_f(t_f) - Y_k^\top(t)D_{4,k}\xi(t) + \epsilon \xi^\top(t)D_{5,k}\xi_f(t_f), \end{aligned} \quad (\text{A.17})$$

where

$$\begin{cases} Q_{k,2}^{ext} = U_{-k}^\top(\mathcal{L}_{k,red}^{ext \top} \mathcal{L}_{k,red}^{ext} \otimes K_k^{ext \top} R_k K_k^{ext})U_{-k}, \\ D_{1,k} = \Psi(\epsilon)^\top \tilde{H}^\top(\mathcal{L}_{k,row}^{ext \top} \mathcal{L}_{k,row}^{ext} \otimes K_k^{ext \top} R_k K_k^{ext})\tilde{H}\Psi(\epsilon), \\ D_{2,k} = \tilde{Z}^\top(\mathcal{L}_{k,row}^{ext \top} \mathcal{L}_{k,row}^{ext} \otimes K_k^{ext \top} R_k K_k^{ext})\tilde{Z}, \\ D_{3,k} = 2U_{-k}^\top(\mathcal{L}_{k,red}^{ext \top} \mathcal{L}_{k,row}^{ext} \otimes K_k^{ext \top} R_k K_k^{ext})\tilde{H}\Psi(\epsilon), \\ D_{4,k} = 2U_{-k}^\top(\mathcal{L}_{k,red}^{ext \top} \mathcal{L}_{k,red}^{ext} \otimes K_k^{ext \top} R_k K_k^{ext})\tilde{Z}, \\ D_{5,k} = 2\tilde{Z}^\top(\mathcal{L}_{k,row}^{ext \top} \mathcal{L}_{k,row}^{ext} \otimes K_k^{ext \top} R_k K_k^{ext})\tilde{H}\Psi(\epsilon). \end{cases}$$

Secondly, let's consider the state part of the external cost. To simplify the expression, we use $(\mathcal{L}_k^{ext} \otimes I_{n_x})\tilde{H}y_s(t) = -(\mathcal{L}_{k,col}^{ext} \otimes I_{n_x})U_{-k}Y_k(t)$ where $\mathcal{L}_{k,col}^{ext}$ is the matrix \mathcal{L}_k^{ext} with its k -th block-column removed. Then, we obtain

$$\begin{aligned} & x^\top(t)(\mathcal{L}_k^{ext} \otimes I_{n_x})x(t) \\ &= \star^\top(\mathcal{L}_k^{ext} \otimes I_{n_x})(\tilde{H}y_s(t) + \epsilon \tilde{H}\Psi(\epsilon)\xi_f(t_f) + \tilde{Z}\xi(t)) \\ &= n_k Y_k^\top(t)Q_{k,1}^{ext}Y_k(t) + \epsilon^2 \xi_f^\top(t_f)M_{1,k}\xi_f(t_f) \\ & + \xi^\top(t)M_{2,k}\xi(t) - \epsilon Y_k^\top(t)M_{3,k}\xi_f(t_f) - Y_k^\top(t)M_{4,k}\xi(t) \\ & + \epsilon \xi^\top(t)M_{5,k}\xi_f(t_f) \end{aligned} \quad (\text{A.18})$$

where

$$\begin{cases} M_{1,k} = \Psi(\epsilon)^\top \tilde{H}^\top(\mathcal{L}_k^{ext} \otimes I_{n_x})\tilde{H}\Psi(\epsilon) \\ M_{2,k} = \tilde{Z}^\top(\mathcal{L}_k^{ext} \otimes I_{n_x})\tilde{Z} \\ M_{3,k} = 2U_{-k}^\top(\mathcal{L}_{k,col}^{ext \top} \otimes I_{n_x})\tilde{H}\Psi(\epsilon) \\ M_{4,k} = 2U_{-k}^\top(\mathcal{L}_{k,col}^{ext \top} \otimes I_{n_x})\tilde{Z} \\ M_{5,k} = 2\tilde{Z}^\top(\mathcal{L}_k^{ext} \otimes I_{n_x})\tilde{H}\Psi(\epsilon). \end{cases}$$

Then, replacing (A.17) and (A.18) into the external cost (J_k^{ext}) in equation (8), we get

$$\begin{aligned} & J_k^{ext}(T, +\infty) \\ &= n_k \int_T^{+\infty} Y_k^\top(t)Q_{k,1}^{ext}Y_k(t) + Y_k^\top(t)\frac{Q_{k,2}^{ext}}{n_k}Y_k(t) dt + \Delta_1 \\ &= n_k \bar{J}_k^{ext}(T, +\infty) + \Delta_1, \end{aligned} \quad (\text{A.19})$$

where $\Delta_1 = \Delta_1^1 + \Delta_1^2 + \Delta_1^3 + \Delta_1^4 + \Delta_1^5$ and

$$\begin{cases} \Delta_1^1 = \epsilon^2 \int_T^{+\infty} \xi_f^\top(t_f)^\top (M_{1,k} + D_{1,k}) \xi_f(t_f) dt, \\ \Delta_1^2 = \int_T^{+\infty} \xi^\top(t) (M_{2,k} + D_{2,k}) \xi(t) dt, \\ \Delta_1^3 = -\epsilon \int_T^{+\infty} Y_k^\top(t) (M_{3,k} + D_{3,k}) \xi_f(t_f) dt, \\ \Delta_1^4 = -\int_T^{+\infty} Y_k^\top(t) (M_{4,k} + D_{4,k}) \xi(t) dt, \\ \Delta_1^5 = \epsilon \int_T^{+\infty} \xi^\top(t) (M_{5,k} + D_{5,k}) \xi_f(t_f) dt. \end{cases} \quad (\text{A.20})$$

$$\begin{aligned} \Delta_1^1 &\leq \epsilon^2 \|M_{1,k} + D_{1,k}\| \int_T^{+\infty} \|\xi_f(t_f)\|^2 dt \\ &\leq -\epsilon^2 \frac{\|M_{1,k} + D_{1,k}\| \|\xi_f(0)\|^2}{2\nu(\bar{A}_{22}^2)} e^{2\nu(\bar{A}_{22}^2)T} = \mathcal{O}(\epsilon^2). \end{aligned}$$

$$\begin{aligned} \Delta_1^2 &\leq \mathbf{C}_{3,k} \|M_{2,k} + D_{2,k}\| \int_T^{+\infty} \|\xi(t)\|^2 \|\xi(T)\|^2 dt \\ &\leq \mathbf{C}_{3,k} \|M_{2,k} + D_{2,k}\| (\|\xi_f(T)\|^2 + 2\mathcal{O}(\epsilon) \|\xi_f(T)\| + \mathcal{O}(\epsilon^2)) \\ &\leq \mathcal{O}(\epsilon^2). \\ \Delta_1^3 &\leq \epsilon \|M_{3,k} + D_{3,k}\| \|Y(0)\| \|\xi_f(0)\| \int_T^{+\infty} e^{\nu(A_{cl})t} e^{\nu(\bar{A}_{22}^2)t} dt \\ &= -\epsilon \frac{\|M_{3,k} + D_{3,k}\| \|Y(0)\| \|\xi_f(0)\|}{\nu(A_{cl}) + \nu(\bar{A}_{22}^2)} e^{(\nu(A_{cl}) + \nu(\bar{A}_{22}^2))T} = \mathcal{O}(\epsilon). \end{aligned}$$

Similarly, Δ_1^4 and Δ_1^5 are of order $\mathcal{O}(\epsilon)$. Finally, from (A.19) and bounds in (A.20) for Δ_1 , we obtain

$$J_k^{ext}(T, +\infty) = n_k \bar{J}_k^{ext}(T, +\infty) + \mathcal{O}(\epsilon). \quad (\text{A.21})$$

Composite term: We rewrite the external control (A.16) and the internal control (6) as

$$\begin{aligned} u_k^{ext}(t) &= -\mathbf{C}_{5,k} Y_k(t) - \epsilon \mathbf{C}_{6,k} \xi_f(t_f) - \mathbf{C}_{7,k} \xi(t) \\ u_k^{int}(t) &= (\mathcal{L}_k^{int} \otimes K_k^{int}) \tilde{Z}_k \xi_k(t) =: \mathbf{C}_{8,k} \xi_k(t). \end{aligned} \quad (\text{A.22})$$

where $\mathbf{C}_{5,k} = (\mathcal{L}_{k,red}^{ext} \otimes K_k^{ext})U_{-k}$, $\mathbf{C}_{6,k} = (\mathcal{L}_{k,row}^{ext} \otimes K_k^{ext})\tilde{H}\Psi(\epsilon)$ and $\mathbf{C}_{7,k} = (\mathcal{L}_{k,row}^{ext} \otimes K_k^{ext})\tilde{Z}$. Then, taking the norm and substituting from equations (A.22) into the J_k^{cross} term in equation (8), we get,

$$\begin{aligned} J_k^{cross}(T, +\infty) &\leq 2\|R_k\| \int_T^{+\infty} \|u_k^{ext \top}(t)\| \|u_k^{int}(t)\| dt \\ &\leq 2\|R_k\| \int_T^{+\infty} \|\mathbf{C}_{5,k} Y_k(t) + \epsilon \mathbf{C}_{6,k} \xi_f(t_f) + \mathbf{C}_{7,k} \xi(t)\| \\ & \quad \|\mathbf{C}_{8,k} \xi_k(t)\| dt \end{aligned} \quad (\text{A.23})$$

With a simple calculation, it can be shown that the first integral in the above equation is of order $\mathcal{O}(\epsilon)$ and the second and the third integrals are of order $\mathcal{O}(\epsilon^2)$. Thus, we have,

$$J_k^{cross}(T, +\infty) \leq \mathcal{O}(\epsilon). \quad (\text{A.24})$$

Finally, from (8), (A.15), (A.21) and (A.24), we conclude the proof.

Proof of Theorem 2

Internal Cost: Following the similar approximation as the approximation of the internal cost in Proposition 3, we obtain the following approximation for the internal cost for

$$J_k^{int} = n_k J_{f,k} + \mathcal{O}(\epsilon) \quad (\text{A.25})$$

Moreover, due to LQ-control design, the optimal fast cost $J_{f,k} = \xi_{f,k}(0)^\top (I_{n_{k-1}} \otimes P_k^{int}) \xi_{f,k}(0)$. The substituting the approximation $\xi_k = \xi_{f,k} + \mathcal{O}(\epsilon)$, we get, $J_{f,k} = \xi_k(0)^\top (I_{n_{k-1}} \otimes P_k^{int}) \xi_k(0) + \mathcal{O}(\epsilon)$. Then, from the transformation (13), it yields,

$$\begin{aligned} J_k^{int} &= n_k \cdot x_k(0)^\top Z_k^\top (I_{n_{k-1}} \otimes P_k^{int}) Z_k x_k(0) + \mathcal{O}(\epsilon) \\ &= x_k(0)^\top (I_{n_k} \otimes P_k^{int}) x_k(0) + \mathcal{O}(\epsilon) \\ &\leq \|P_k^{int}\| \|x_k(0)\|^2 + \mathcal{O}(\epsilon). \end{aligned} \quad (\text{A.26})$$

External Cost: Substituting $x_k = \tilde{H}y + \tilde{Z}\xi$ in the external cost J_k^{ext} in equation (8), and performing the similar operation as in the approximation of the external cost in Proposition 3, we obtain,

$$J_k^{ext} \leq n_k \bar{J}_k^{ext} + \Pi_1 + \mathcal{O}(\epsilon) \quad (\text{A.27})$$

with

$$\begin{aligned} \Pi_1 = & 2 \int_0^{+\infty} \xi^\top \tilde{Z}^\top ((\mathcal{L}_k^{ext} \otimes I_{n_x}) + \\ & (\mathcal{L}_{k,row}^{ext} \mathcal{L}_{k,row}^{ext} \otimes K_k^{ext} R_k K_k^{ext})) \tilde{H} y dt \\ & + \int_0^{+\infty} \xi^\top (\tilde{Z}^\top (\mathcal{L}_k^{ext} \otimes I_{n_x}) \\ & + (\mathcal{L}_{k,row}^{ext} \mathcal{L}_{k,row}^{ext} \otimes K_k^{ext} R_k K_k^{ext}) \tilde{Z}) \xi dt. \end{aligned} \quad (\text{A.28})$$

Furthermore, substituting $(\mathcal{L}_k^{ext} \otimes I_{n_x}) \tilde{H} y_s = -(\mathcal{L}_{k,col}^{ext} \otimes I_{n_x}) U_{-k} Y_k$ and $(\mathcal{L}_{k,row}^{ext} \otimes I_{n_x}) \tilde{H} y_s = -(\mathcal{L}_{k,red}^{ext} \otimes I_{n_x}) U_{-k} Y_k$ in equation (A.28) and taking the norm we have,

$$\Pi_1 \leq \mathbf{C}_{9,k} \|x(0)\|^2 + \mathcal{O}(\epsilon) \quad (\text{A.29})$$

where $\mathbf{C}_{9,k} := \mathbf{C}_4 \|Z\| (\|Y_k(0)\| \|2\tilde{Z}^\top ((\mathcal{L}_{k,col}^{ext} \otimes I_{n_x}) + (\mathcal{L}_{k,row}^{ext} \mathcal{L}_{k,red}^{ext} \otimes K_k^{ext} R_k K_k^{ext})) U_{-k}\| + \|(\tilde{Z}^\top (\mathcal{L}_k^{ext} \otimes I_{n_x}) + (\mathcal{L}_{k,row}^{ext} \mathcal{L}_{k,row}^{ext} \otimes K_k^{ext} R_k K_k^{ext}) \tilde{Z}) \mathbf{C}_4$.

Cross Term: Substituting from equation (A.22) and from Theorem 1 into the cross term in equation (8) and after further calculation, we get,

$$\begin{aligned} J_k^{cross} \leq & 2 \|R_k\| \|\mathbf{C}_{5,k}\| \|\mathbf{C}_{8,k}\| \|\mathbf{C}_4\| \|Y_k(0)\| \|Z\| \|x(0)\| \\ & + 2 \|R_k\| \|\mathbf{C}_{7,k}\| \|\mathbf{C}_{8,k}\| \|\mathbf{C}_4\| \|Z\|^2 \|x(0)\|^2 + \mathcal{O}(\epsilon) \end{aligned}$$

By definition of the variable Y_k in equation (40), it satisfies $\|Y_k\| \leq \sqrt{n_k} \|H\| \|x(0)\| + \mathcal{O}(\epsilon)$ and substituting it in the above equation leads to

$$J_k^{cross} \leq \mathbf{C}_{10,k} \|x(0)\|^2 + \mathcal{O}(\epsilon), \quad (\text{A.30})$$

where $\mathbf{C}_{10,k} := 2 \|R_k\| \|\mathbf{C}_{8,k}\| \|\mathbf{C}_4\| (\sqrt{n_k} \|H\| \|\mathbf{C}_{5,k}\| + \|\mathbf{C}_{7,k}\| \|Z\|) \|Z\|$. Then from equation (8), (A.26), (A.27), (A.29) and (A.30), we have,

$$J_k \leq \|P_k^{int}\| \|x_k(0)\|^2 + n_k \bar{J}_k^{ext} + \mathbf{C}_k \|x(0)\|^2 + \mathcal{O}(\epsilon)$$

where $\mathbf{C}_k := (\mathbf{C}_{9,k} + \mathbf{C}_{10,k})$. Moreover, we have $\|Y_k(0)\| \leq \|x(0)\|^2 + \mathcal{O}(\epsilon)$ and substituting from equation (45),

$$\begin{aligned} J_k \leq & \|P_k^{int}\| \|x_k(0)\|^2 + n_k \gamma_k \|x(0)\|^2 + \mathbf{C}_k \|x(0)\|^2 + \mathcal{O}(\epsilon) \\ \leq & (\|P_k^{int}\| + n_k \gamma_k + \mathbf{C}_k) \|x(0)\|^2 + \mathcal{O}(\epsilon). \end{aligned} \quad (\text{A.31})$$



Bikash Adhikari obtained his Bachelor's degree in Mechanical Engineering from Motilal Nehru National Institute of Technology (MNNIT), Allahabad, India in 2014 and Master's in Erasmus Mundus Dual Masters in Mathematical Modeling (MATHMODS) from University of L'Aquila, Italy and University of Hamburg, Germany in 2018. Currently, he received his Ph.D. in Automatic Control at CRAN

UMR 7039, CNRS in Nancy, France in 2022. His areas of research include consensus/synchronization of multi-agent systems, distributed control, and singularly perturbed systems.



Jomphop Veetaseveera obtained his M.Sc. in Electrical Engineering and Computer Science from Université du Québec à Chicoutimi (UQAC), Canada in 2017 and M.Sc in Electrical and Control Engineering from École Nationale Supérieure d'Électricité et de Mécanique (ENSEM),

France in 2017. He received his Ph.D. in Automatic Control at CRAN UMR 7039, CNRS in Nancy, France in 2021. His areas of research include consensus/synchronization of multi-agent systems, game theory, distributed control, and singularly perturbed systems.



Vineeth S Varma obtained his Bachelor's in Physics with Honors from Chennai Mathematical Institute, India in 2008, his dual Masters in Science and Technology from Friedrich-Schiller-University of Jena in 2009 and Warsaw University of Technology in 2010. He was awarded his Ph.D. from LSS/Supélec on energy-efficient wireless telecommunications. He did one year

of post-doctoral research at the Singapore University of Technology and Design from 2014-2015. Since 2016, he is a CNRS researcher at CRAN UMR 7039 CNRS in Nancy, France since 2016. His areas of interest are analysis, control, and games over various networks.



Irinel-Constantin Morărescu is currently Professor at Université de Lorraine and a researcher at CRAN UMR 7039 CNRS in Nancy, France. He received the B.S. and the M.S. degrees in Mathematics from the University of Bucharest, Romania, in 1997 and 1999, respectively. In 2006 he received the Ph.D. degree in Mathematics and in Technology of Information and Systems from the University of Bucharest and University

of Technology of Compiègne, respectively. He received the "Habilitation à Diriger des Recherches" from the Université de Lorraine in 2016. His works concern stability and control of time-delay systems, stability and tracking for different classes of hybrid systems, consensus, and synchronization problems.



Elena Panteley received the M.Sc. and Ph.D. degrees in applied mathematics from the State University of St. Petersburg, St. Petersburg, Russia, in 1986 and 1997, respectively. From 1986 to 1998, she held a research position with the Institute for Mechanical Engineering, Russian Academy of Science, St. Petersburg. Since 2004 she holds a tenure position as a Senior Researcher at the French National Centre of

Scientific Research (CNRS), at the Laboratoire de signaux et systèmes, France. She is also an associate researcher at ITMO University, St Petersburg Russia, since 2014. Her research interests include stability and control of nonlinear dynamical systems, and network systems with applications to electromechanical and neuronal systems.